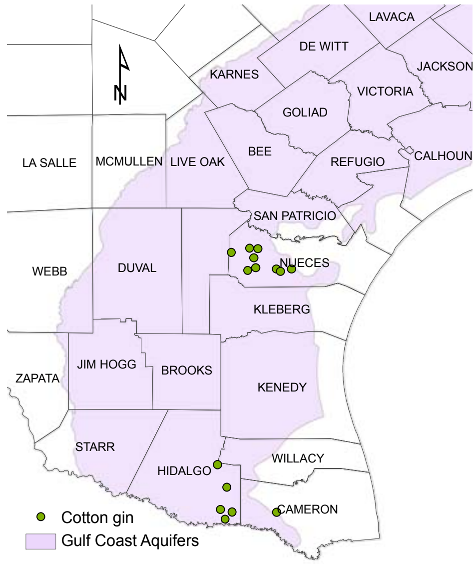

Figure 27. Cotton gin locations in the southwestern Gulf Coast

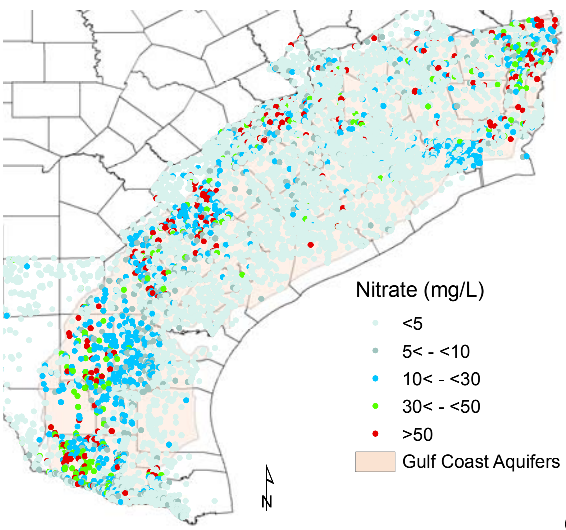

(a)

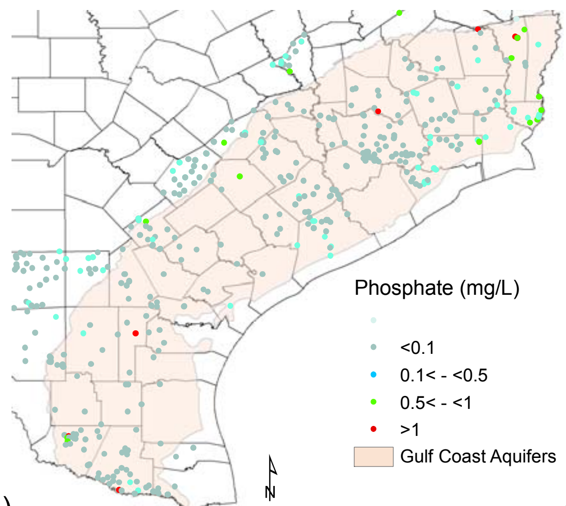

(b)

Figure 28. Nitrate (a) and phosphate (b) distribution in the Gulf Coast

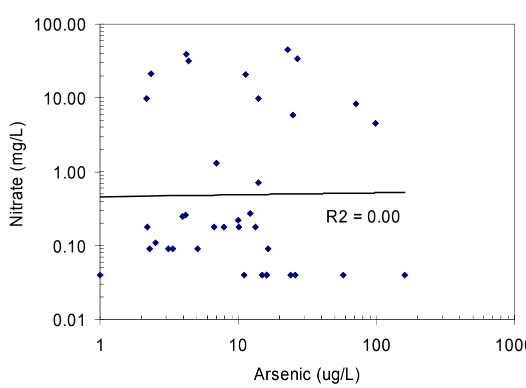

(a)

NOTE: TWDB data (a)

Figure 29. Crossplot of As vs. Nitrate (southwestern Gulf Coast)

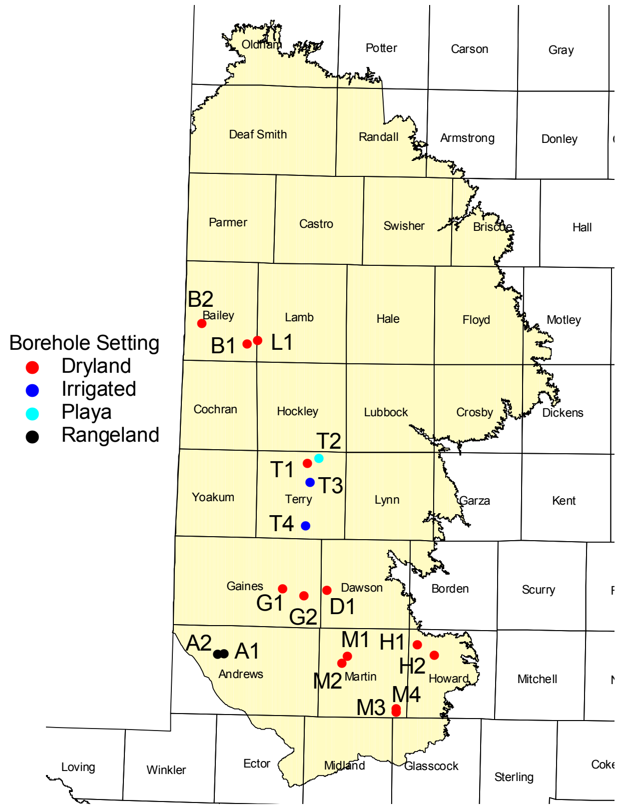

(a)

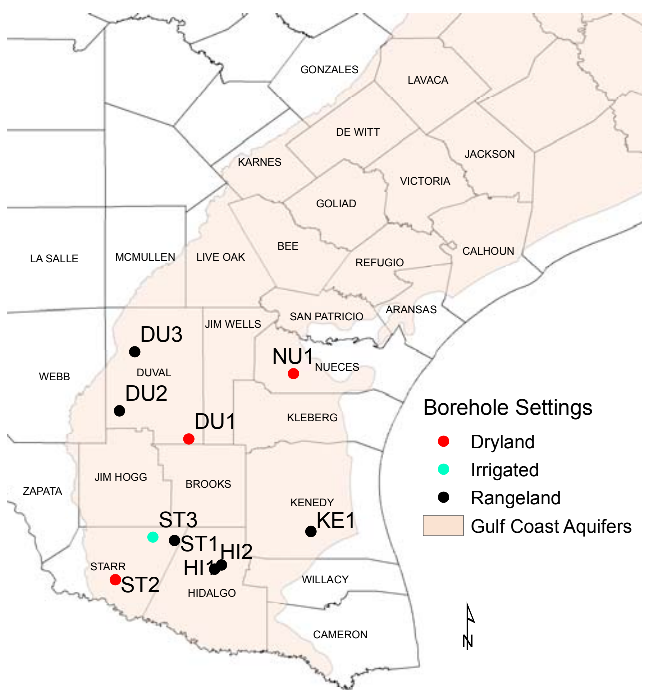

(b)

Figure 30. Drilling sites locations: High Plains (a) and southwestern Gulf Coast (b)

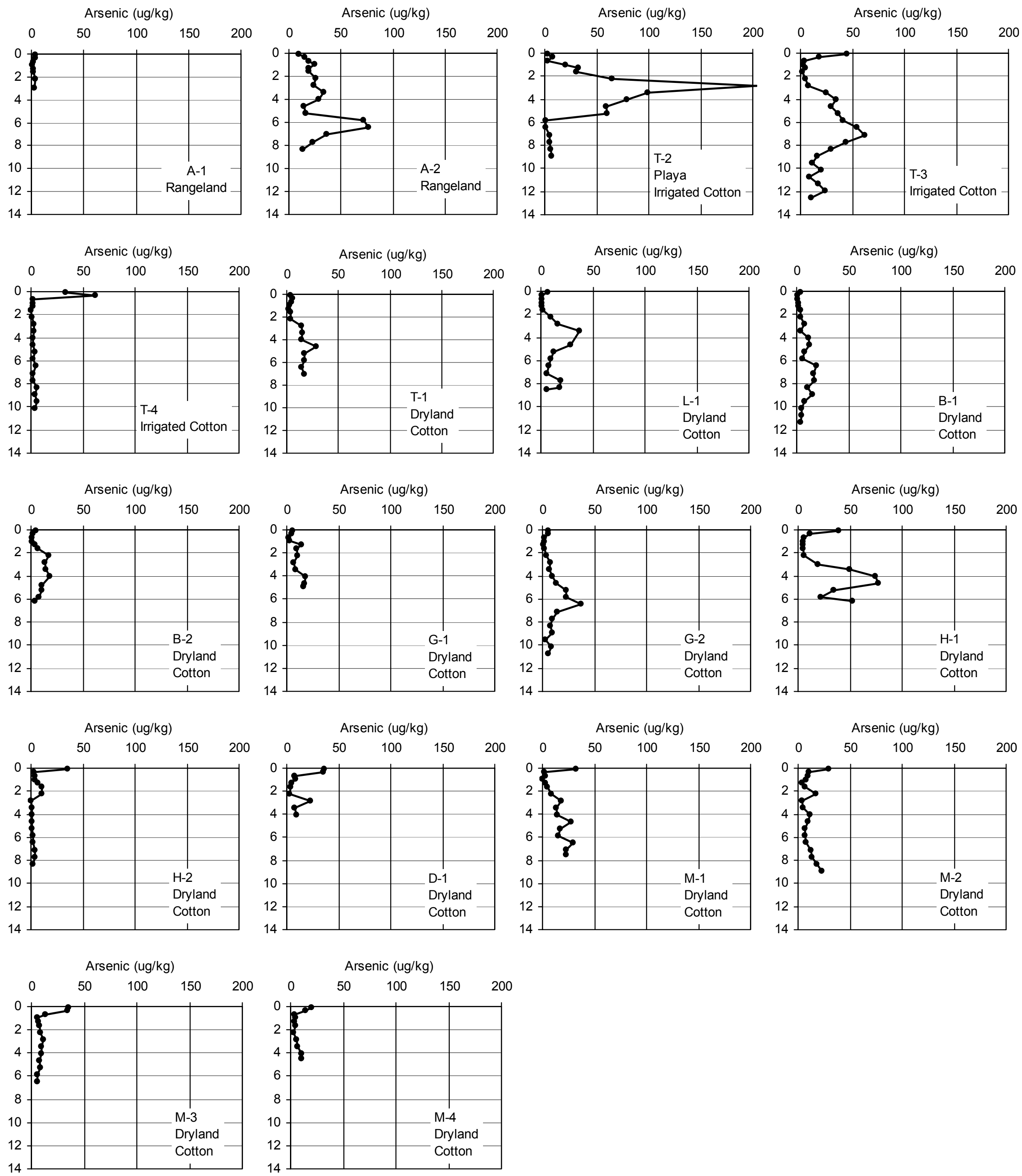

Figure 31. Borehole sample arsenic concentrations in soil in the southern High Plains
.

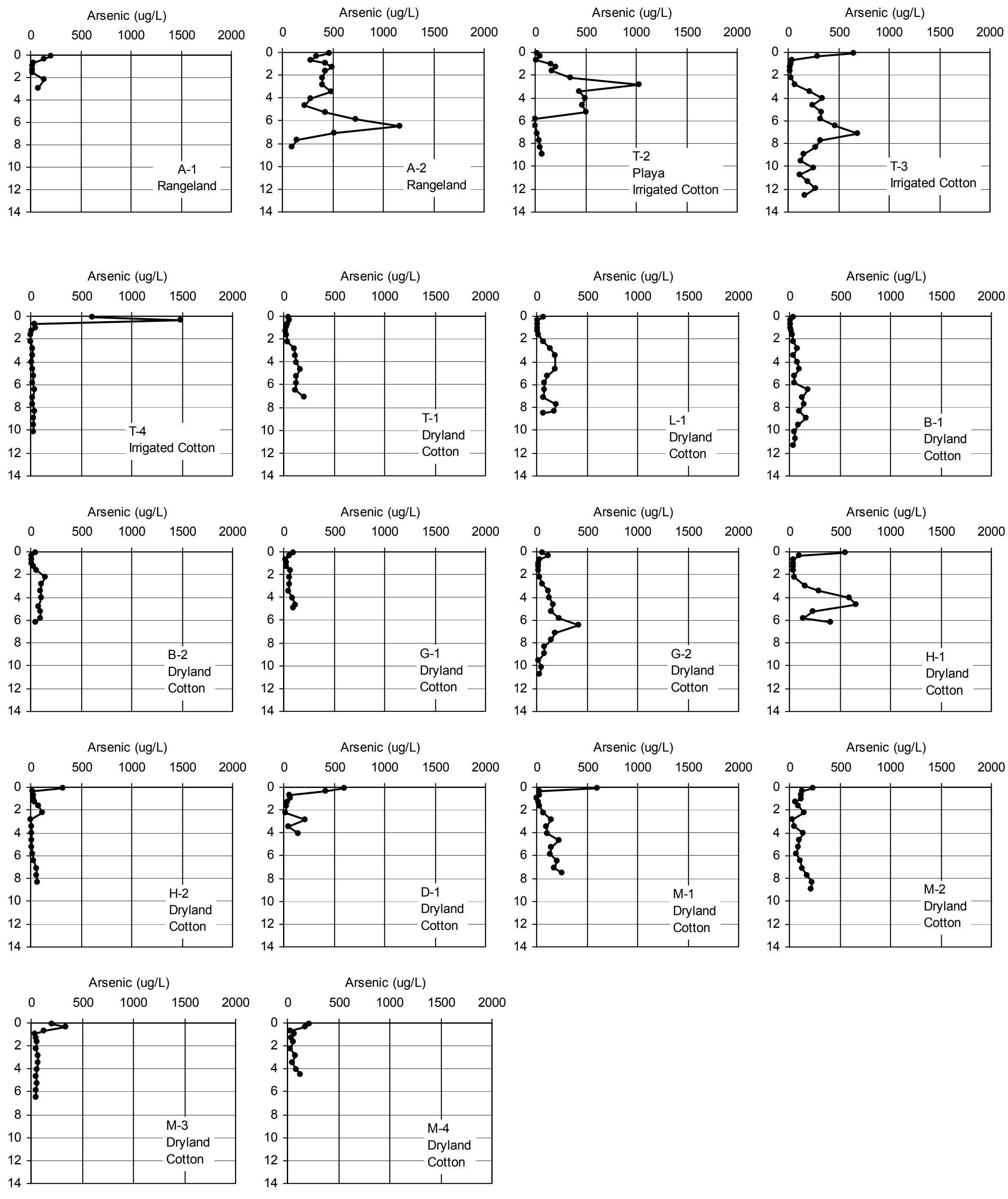

Figure 32. Borehole sample arsenic concentrations in soil water in the southern High Plains
.

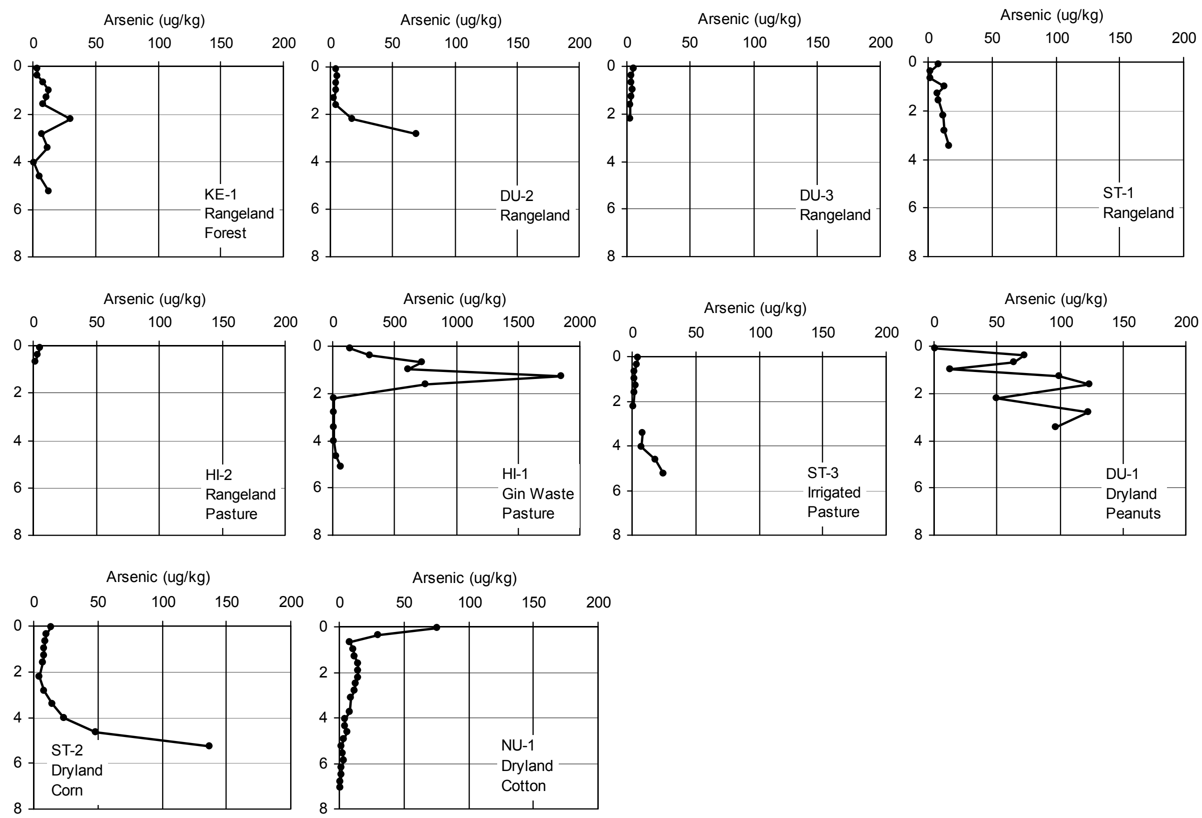

Figure 33. Borehole sample arsenic concentrations in soil in the southwestern Gulf Coast

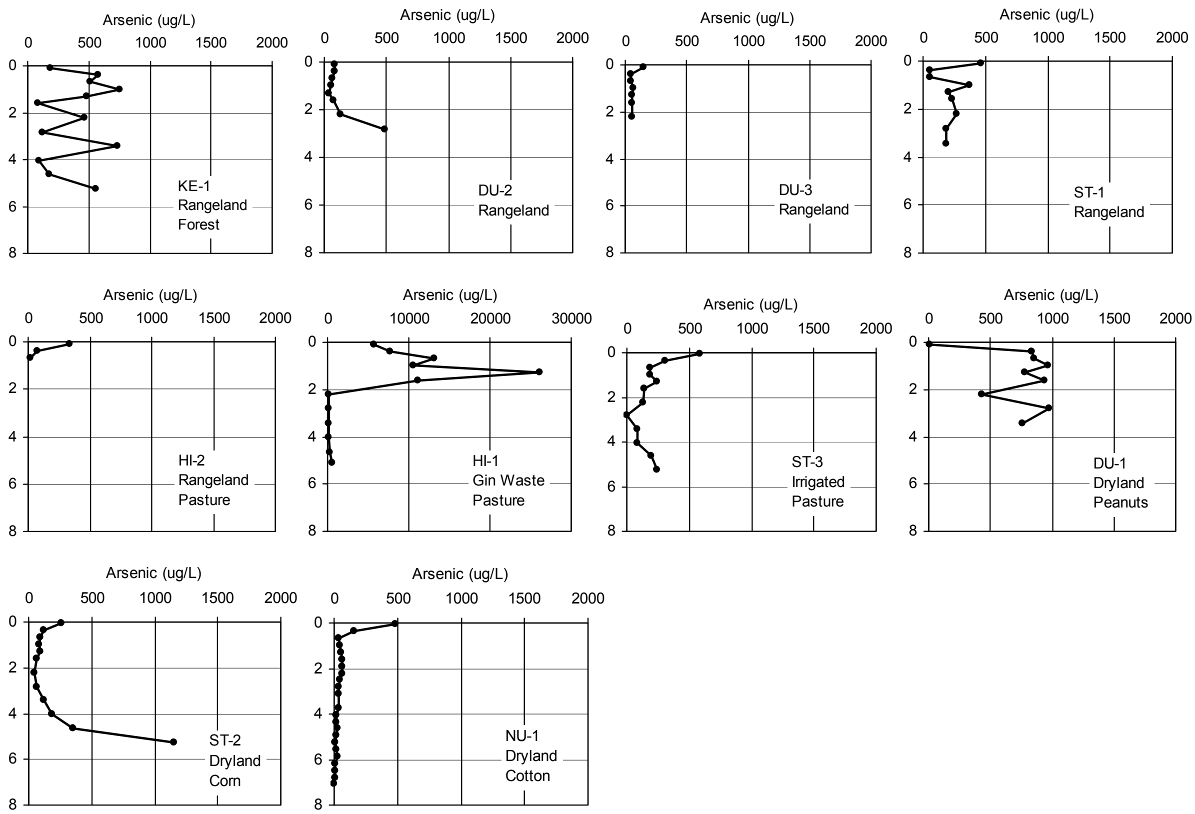

Figure 34. Borehole sample arsenic concentrations in soil water in the southwestern Gulf Coast

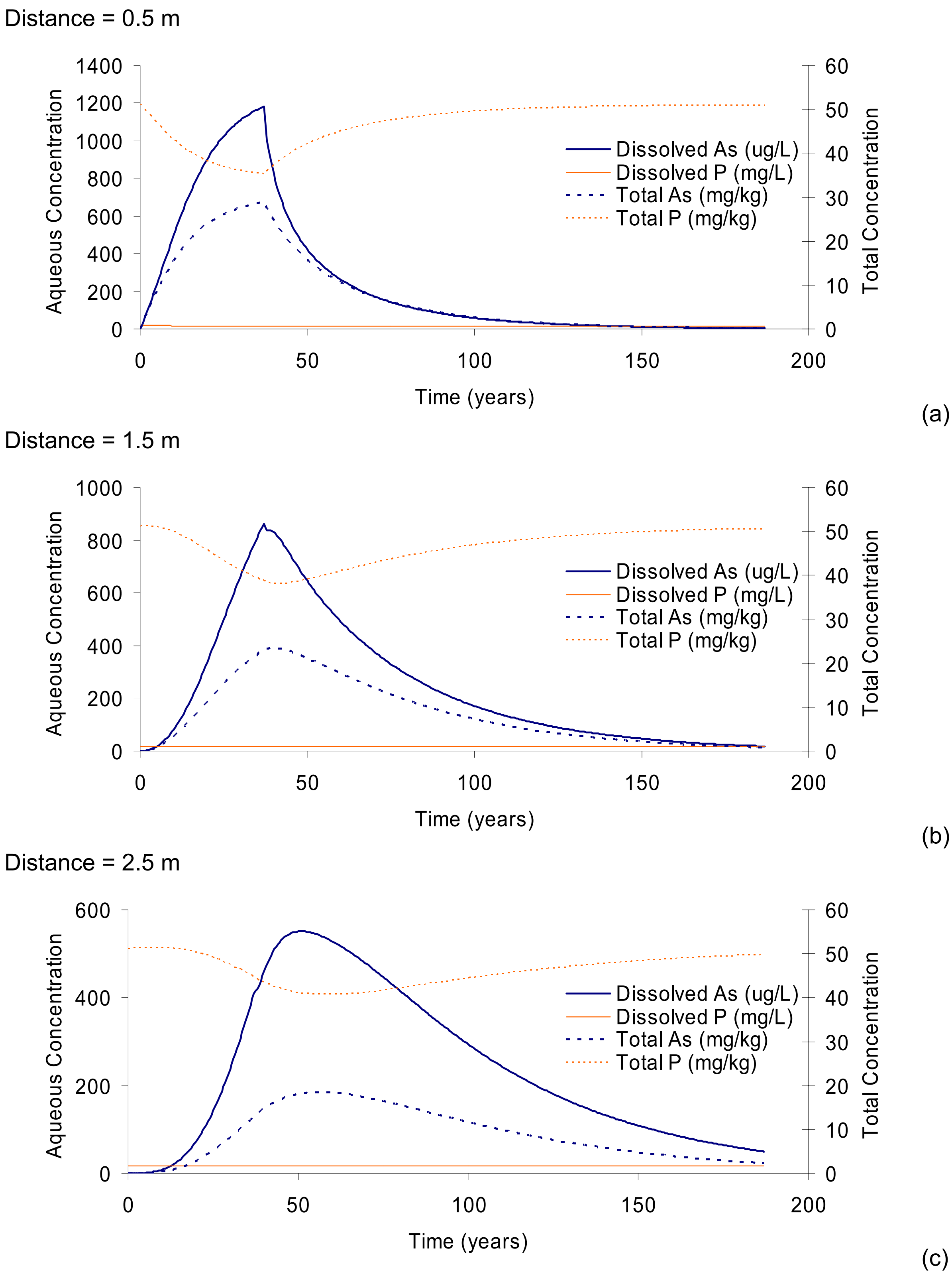

Figure 35. Soil modeling results with phosphates: As and P breakthrough curves at selected distances

Distance = 0.5 m

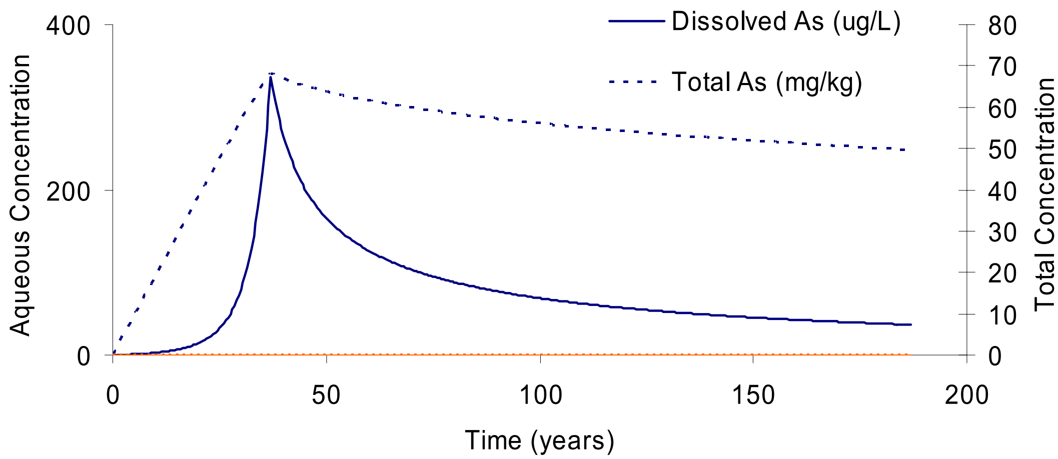

(a)

Distance = 1.5 m

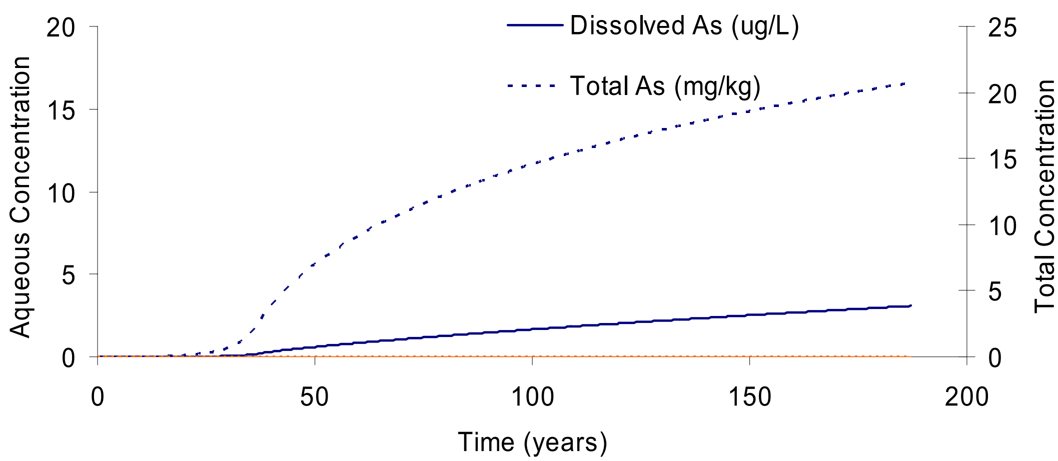

(b)

Distance = 2.5 m

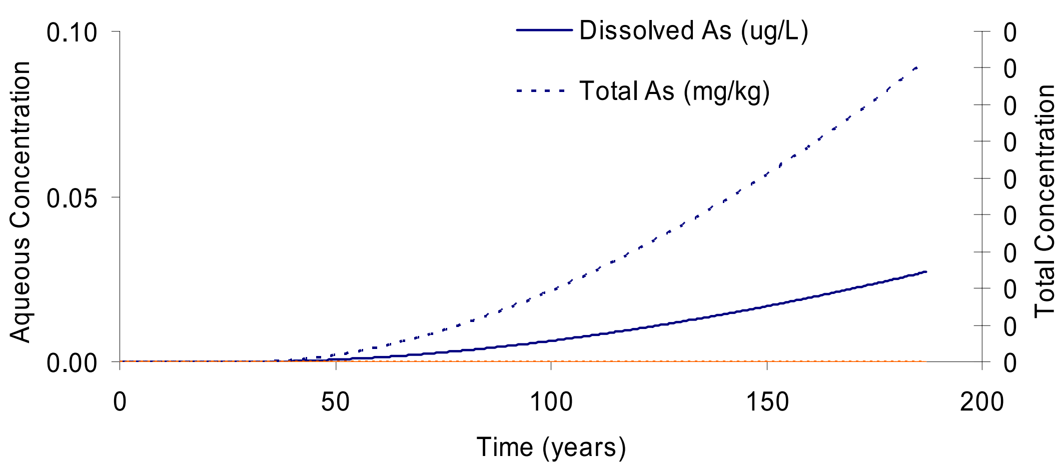

(c)

Figure 36. Soil modeling results without phosphates: As breakthrough curves at selected distances

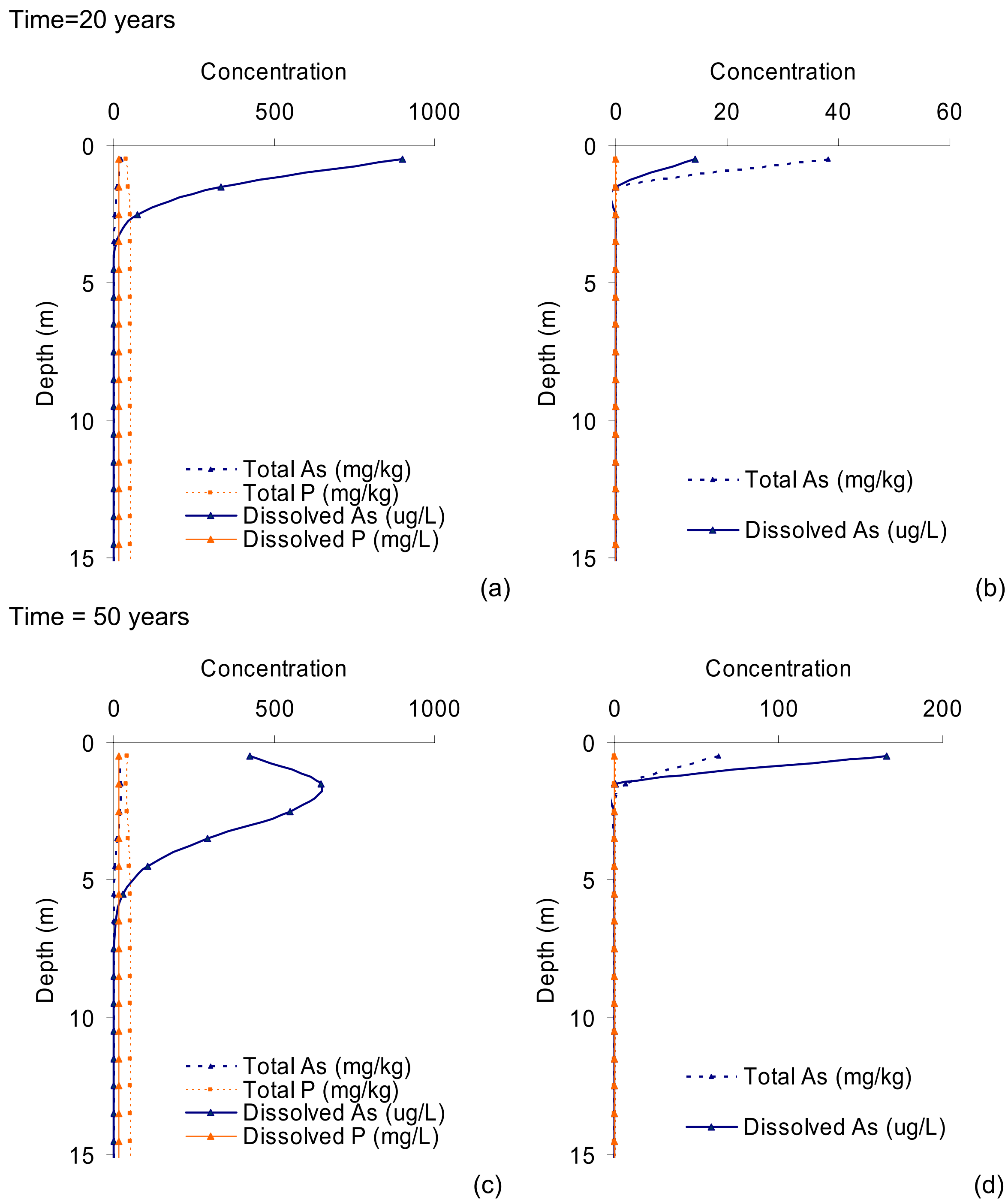

Figure 37. Soil modeling results with and without phosphates: As and P vertical profiles at selected times

Time = 100 years

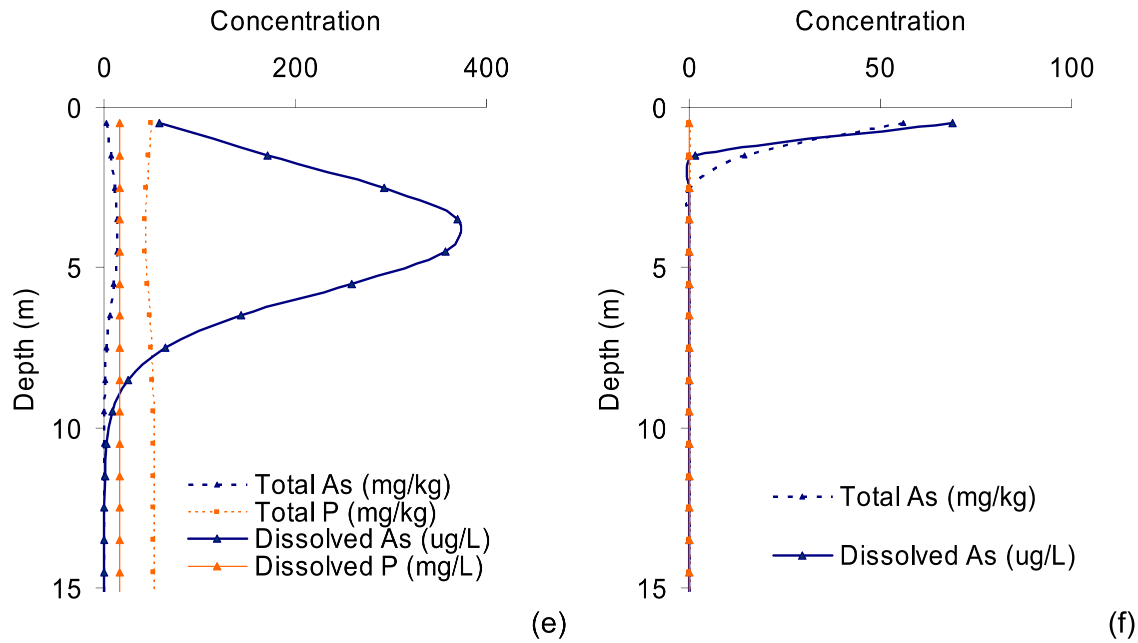

Time = 180 years

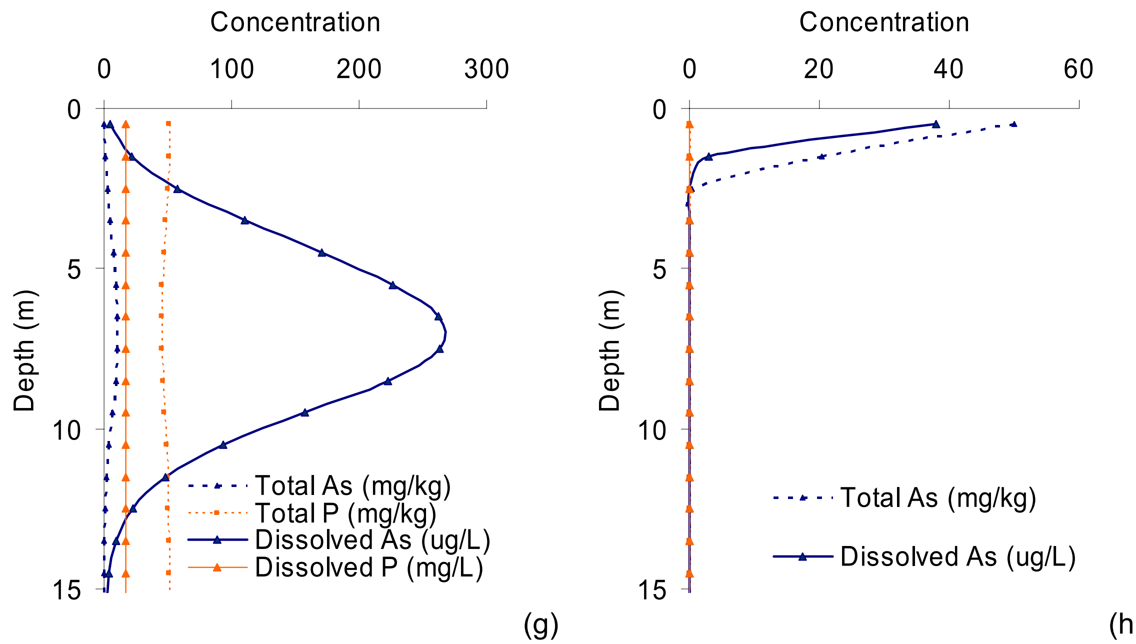

Figure 37. Soil modeling results with and without phosphates: As and P vertical profiles at selected times (continued)

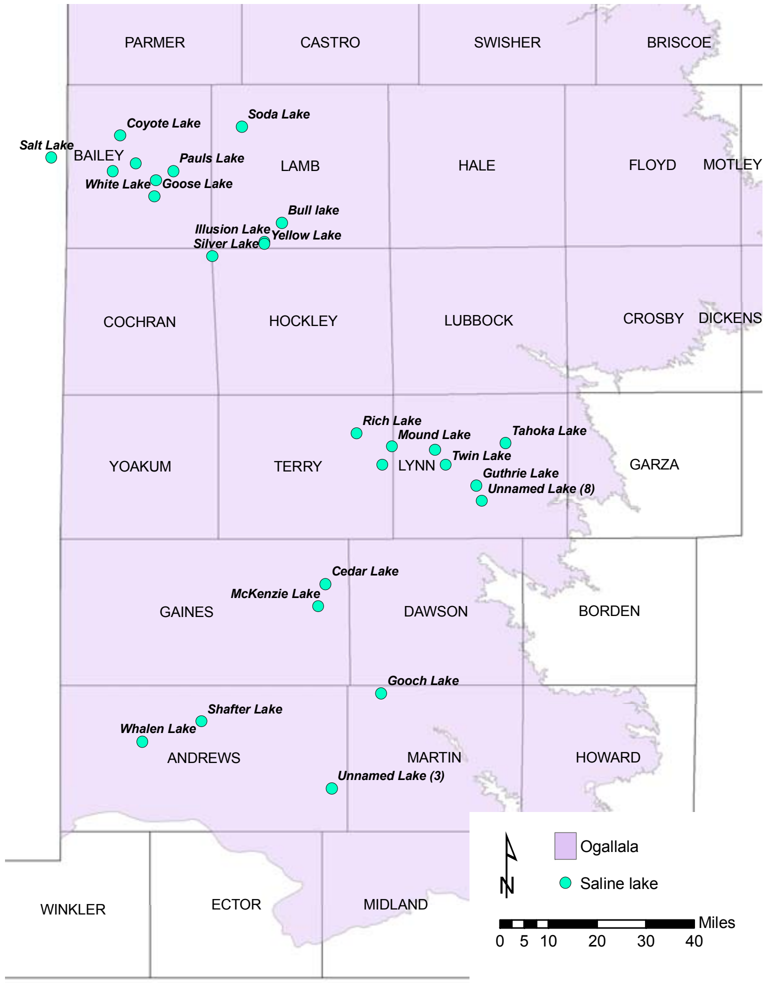

NOTE: Numerals for lakes with unknown lakes are from Wood and Jones (1990)
SOURCE: from Wood and Jones, 1990, and GAT sheets

Figure 38. Location of saline lakes in the Texas High Plains

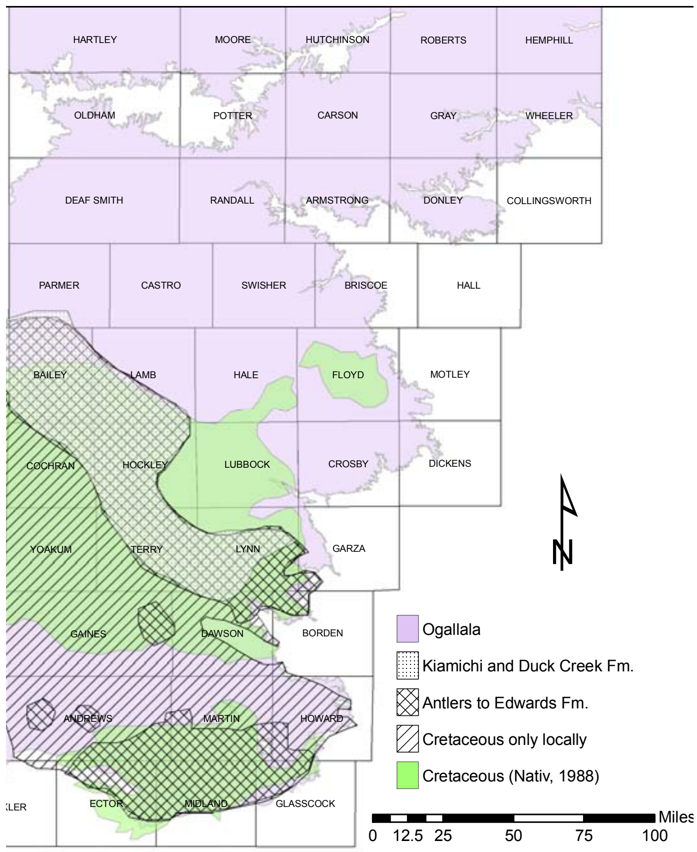

NOTE: Boundaries close to that of Nativ (1988) were adopted by the TWDB as High Plains Edwards-Trinity minor aquifer

SOURCE: (a) Brand et al. (1953) and (b) Nativ (1988)

Figure 39. Location of Cretaceous subcrops in the southern High Plains

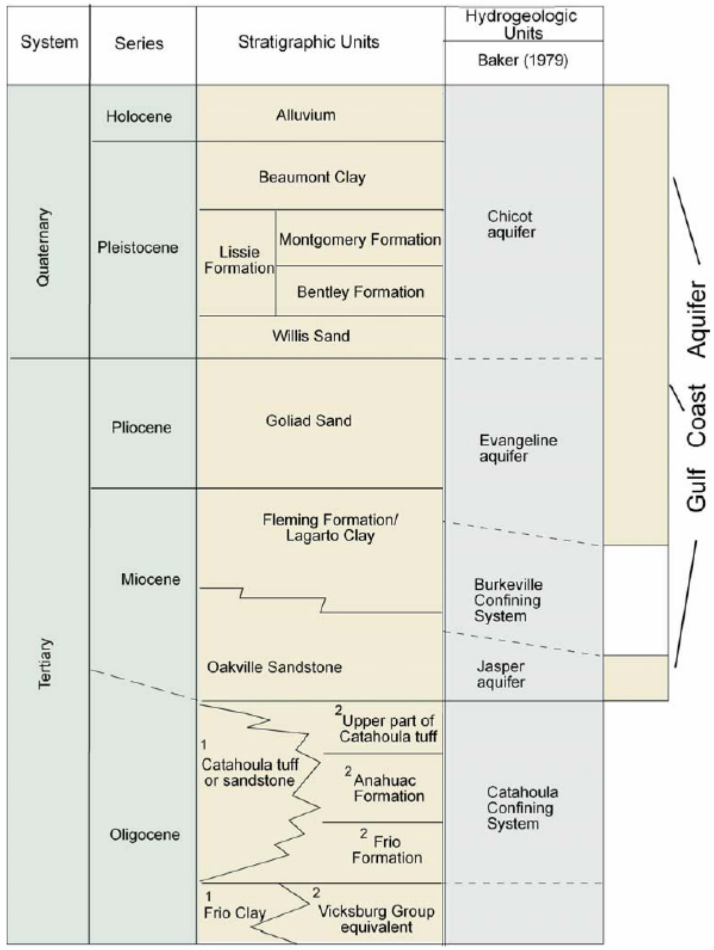

SOURCE: Chowdhury and Mace, 2003

Figure 40. Stratigraphy and hydrostratigrphy of the Gulf Coast aquifers

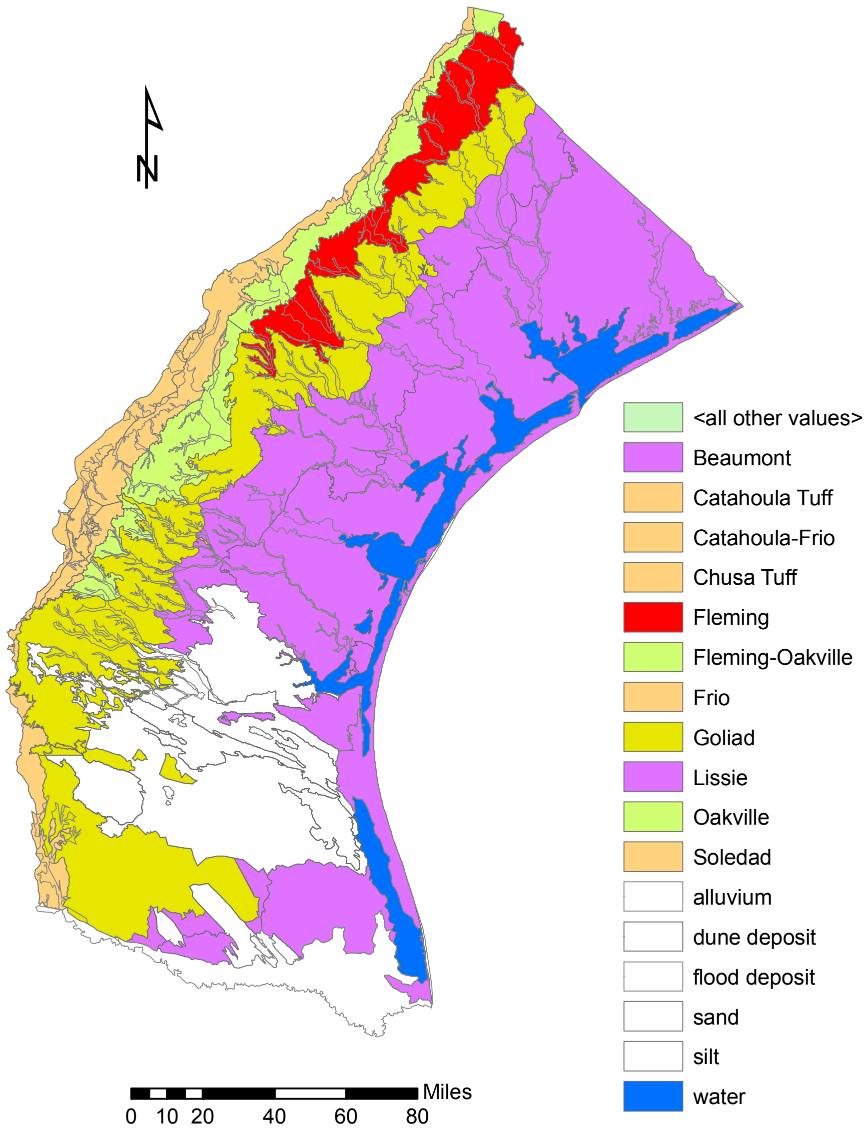

Figure 41. Simplified geologic map of the southwestern Gulf Coast region

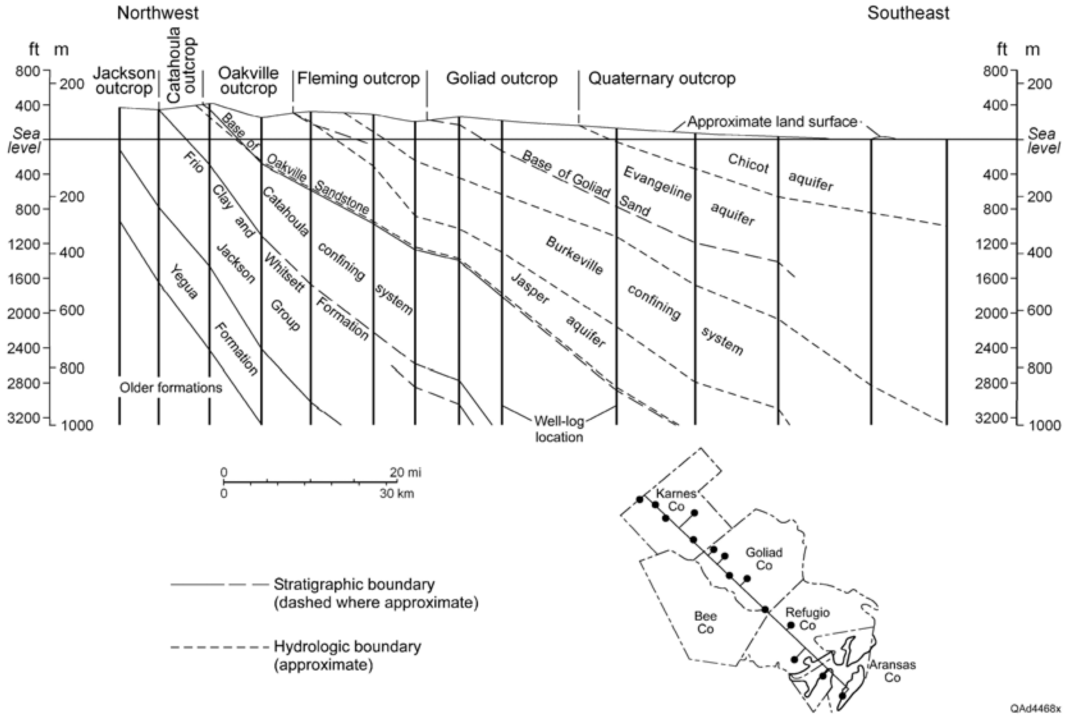

Figure 42. Cross-section along dip in the Gulf Coast aquifer through Karnes, Goliad, and Refugio Counties

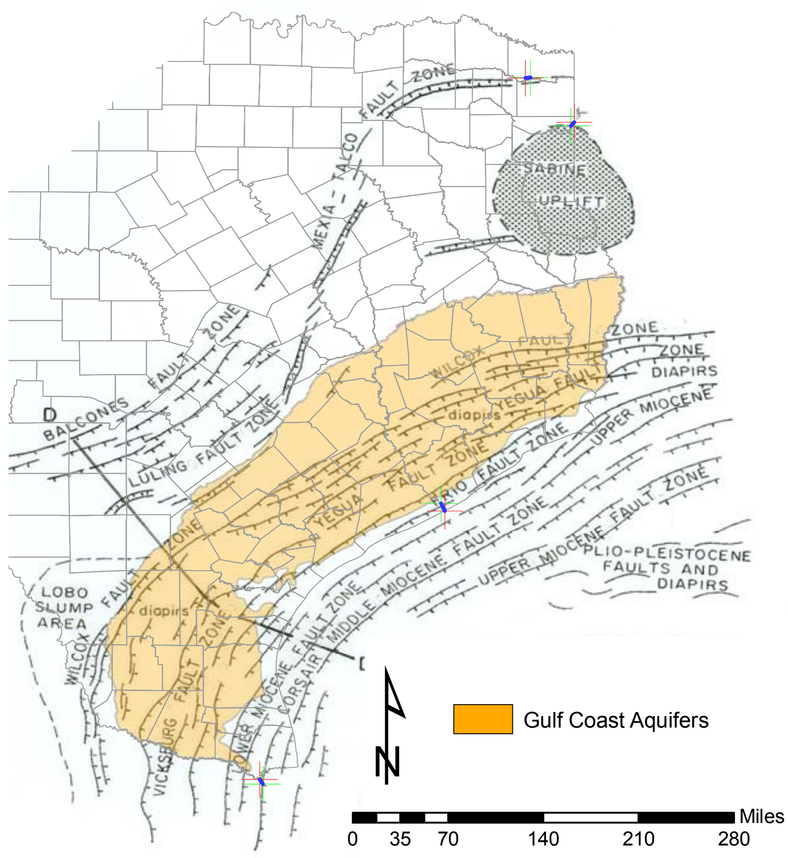

Figure 43. Tectonic map of the Gulf Coast area

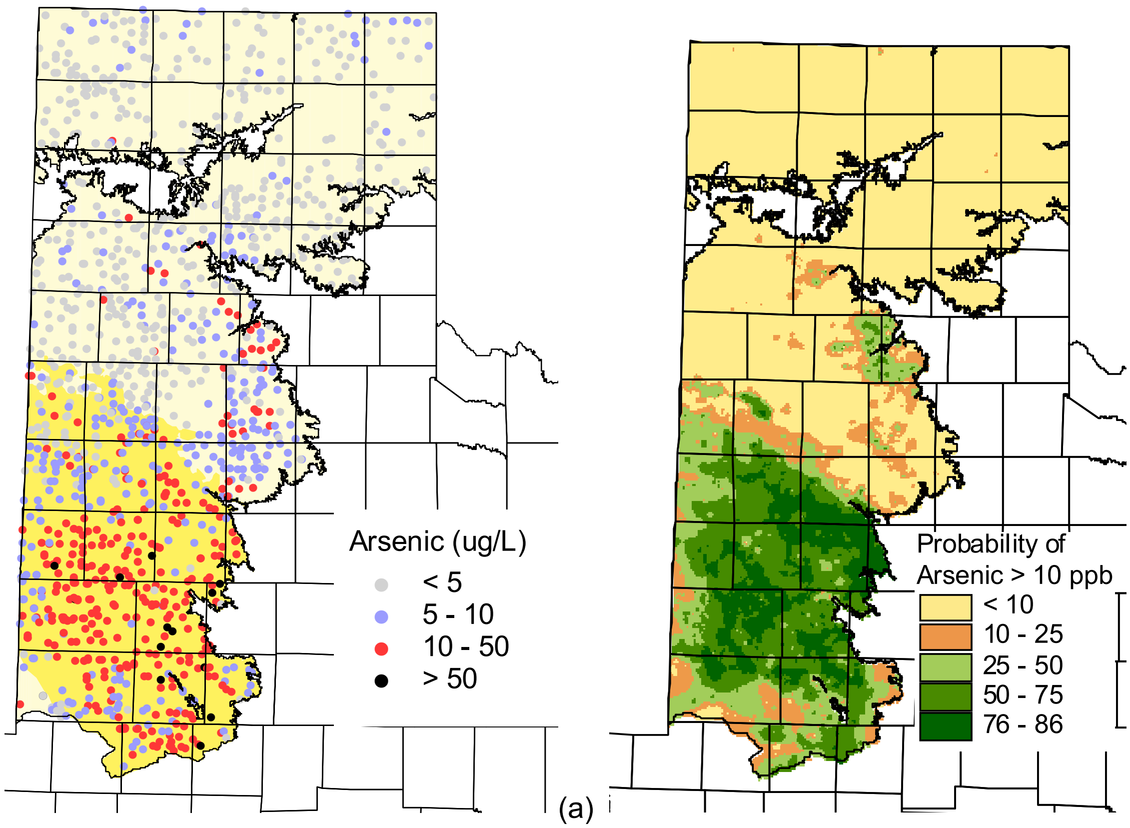

Figure 44. Arsenic distribution in the High Plains aquifer (TWDB database): (a) from arsenic data points; (b) inferred from fluoride data points.

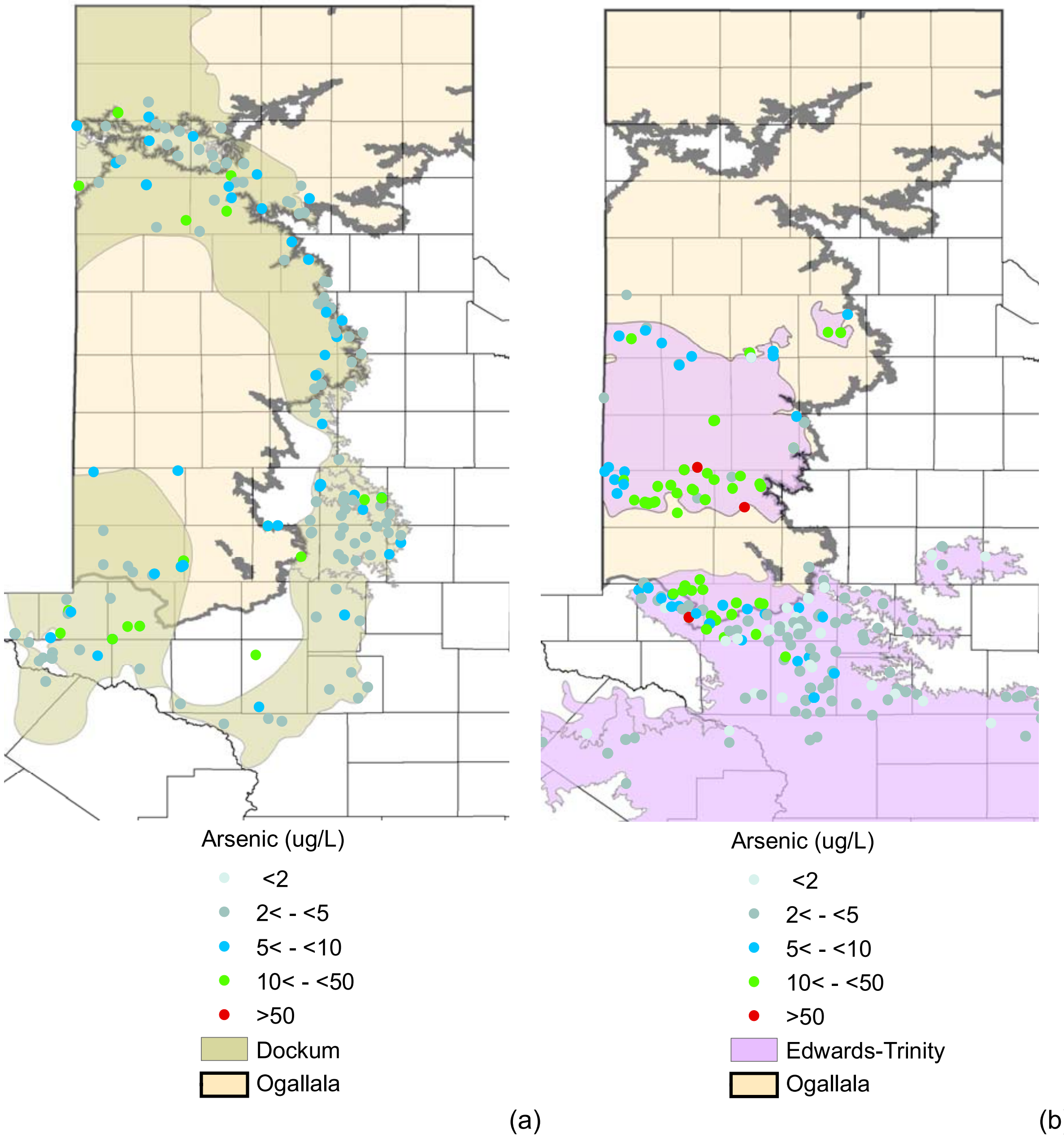

NOTE: data include those High Plains wells screening in multiple formations
NOTE: only Dockum outcrop and that part of the aquifer with a TDS<5,000 mg/L are shown. Downdip central section is more saline. Dockum Fm. underlies all of the southern High Plains aquifer.
SOURCE: aquifer outlines from TWDB GIS coverage of major and minor aquifers

Figure 45. Arsenic distribution in the Dockum (a), Edwards Trinity (b), and Cenozoic Pecos Alluvium aquifers (c).

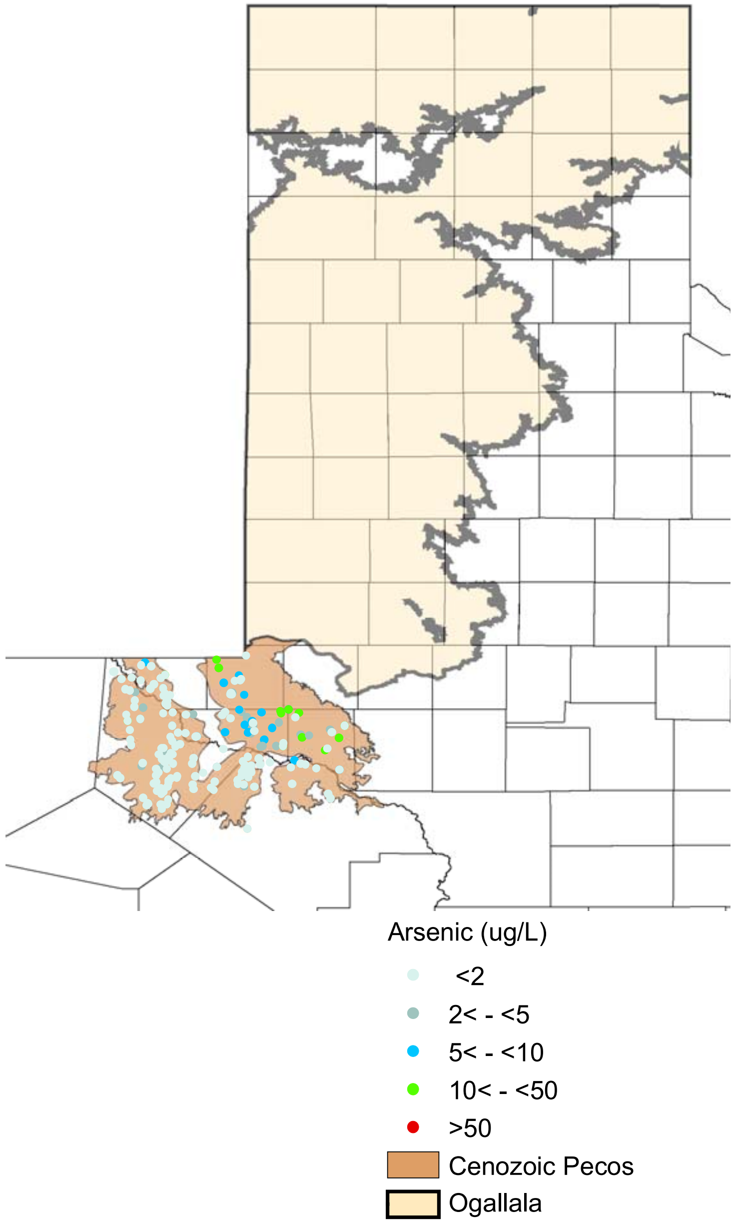

NOTE: data include those High Plains wells screening in multiple formations
SOURCE: aquifer outlines from TWDB GIS coverage of major aquifers
Figure 45. Arsenic distribution in the Dockum (a), Edwards Trinity (b), and Cenozoic Pecos Alluvium aquifers (c). (continued)

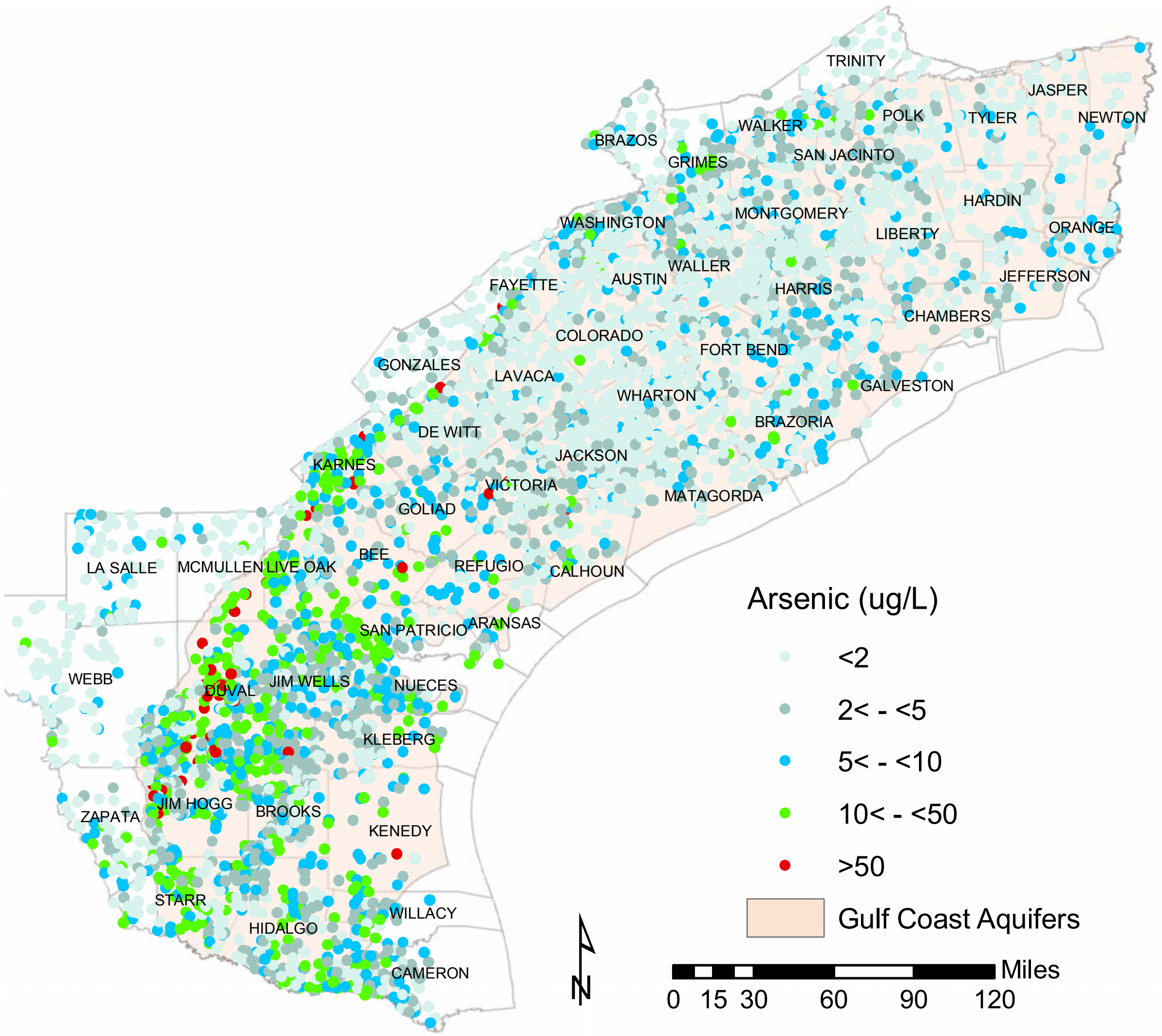

Figure 46. Arsenic distribution in the Gulf Coast aquifers (TWDB and NURE databases)

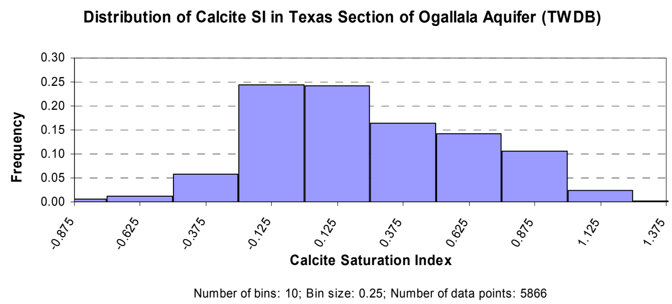

Figure 47. Distribution of calcite saturation index in the southern High Plains aquifer (TWDB data set)

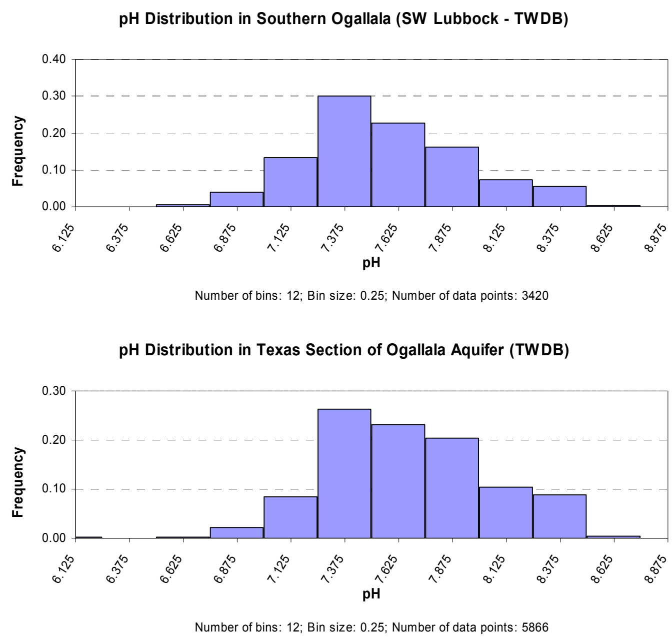

(a)

(b)

Figure 48. pH distribution in the High Plains Aquifer: all Texas data points (a); southwestern region of southern High Plains (b). all data points (TWDB database).

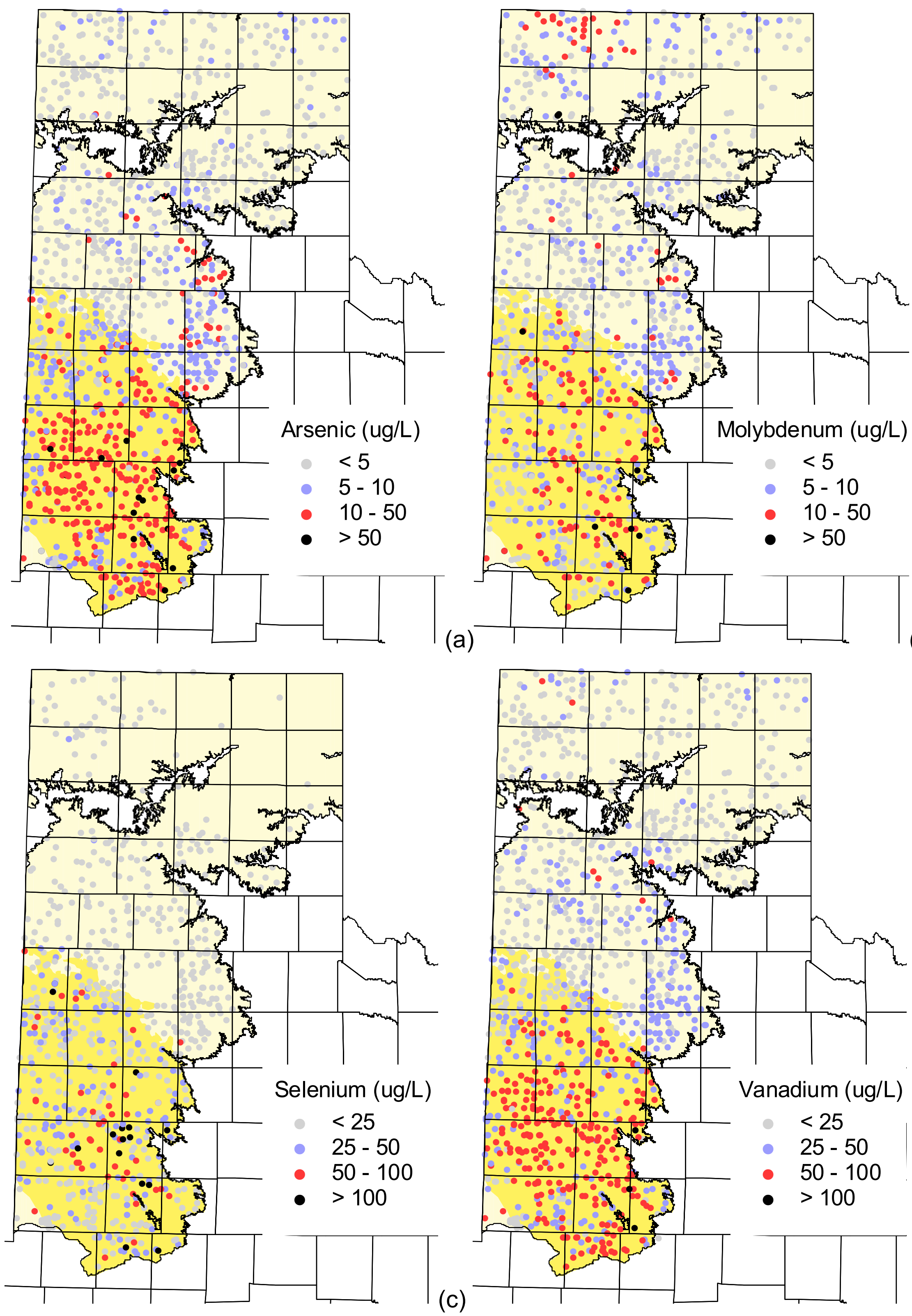

Figure 49. Spatial distribution of As (a), Mo (b), Se (c), V (d), B (e), F (f), U (g), silica (h), Fe (i), chloride (j), sulfate (k), TDS (l), and pH (m) in High Plains aquifers. All plots use only TWDB data except U where NURE data are used.

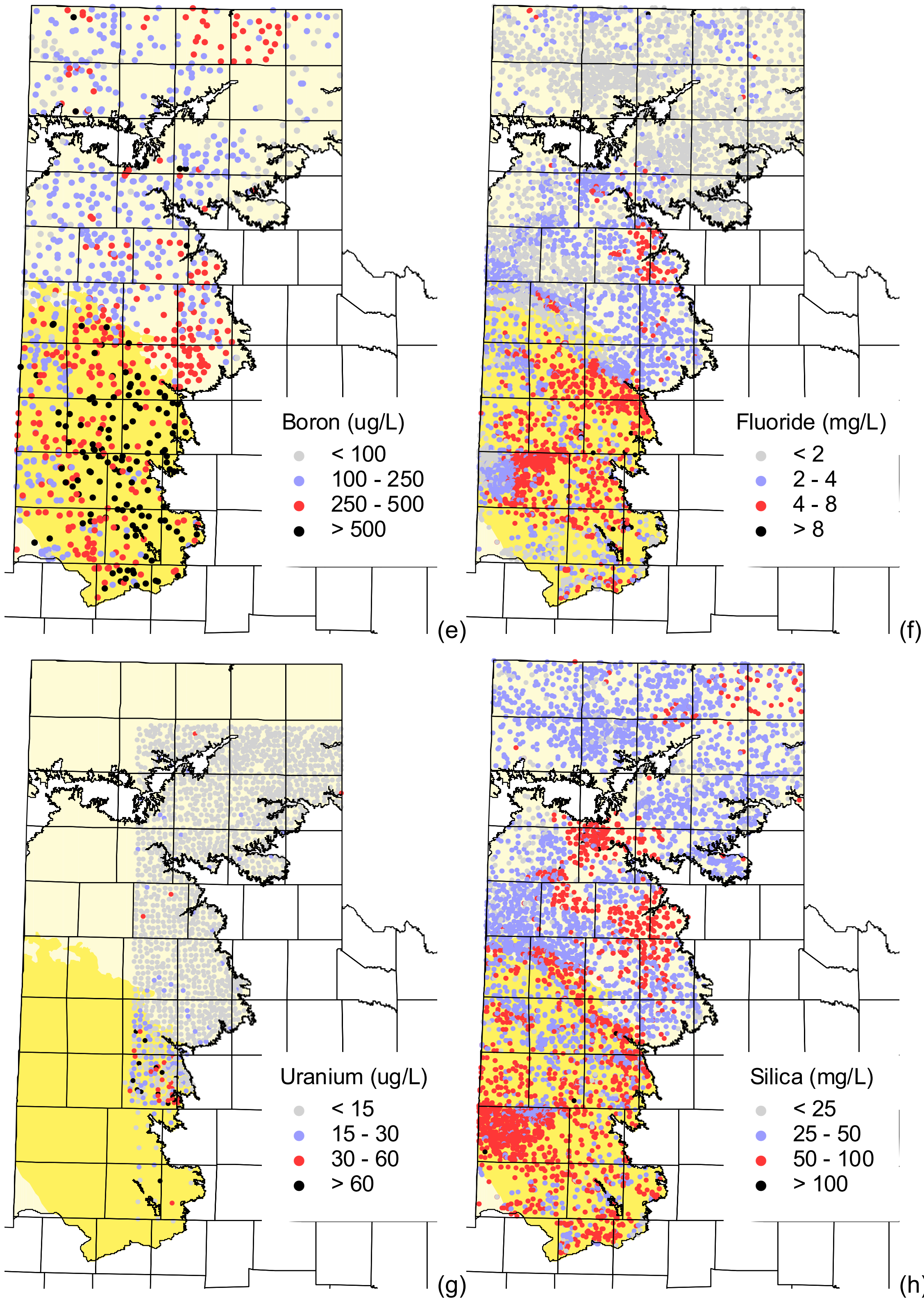

Figure 49. Spatial distribution of As (a), Mo (b), Se (c), V (d), B (e), F (f), U (g), silica (h), Fe (i), chloride (j), sulfate (k), TDS (l), and pH (m) in High Plains aquifers. All plots use only TWDB data except U where NURE data are used. (continued)

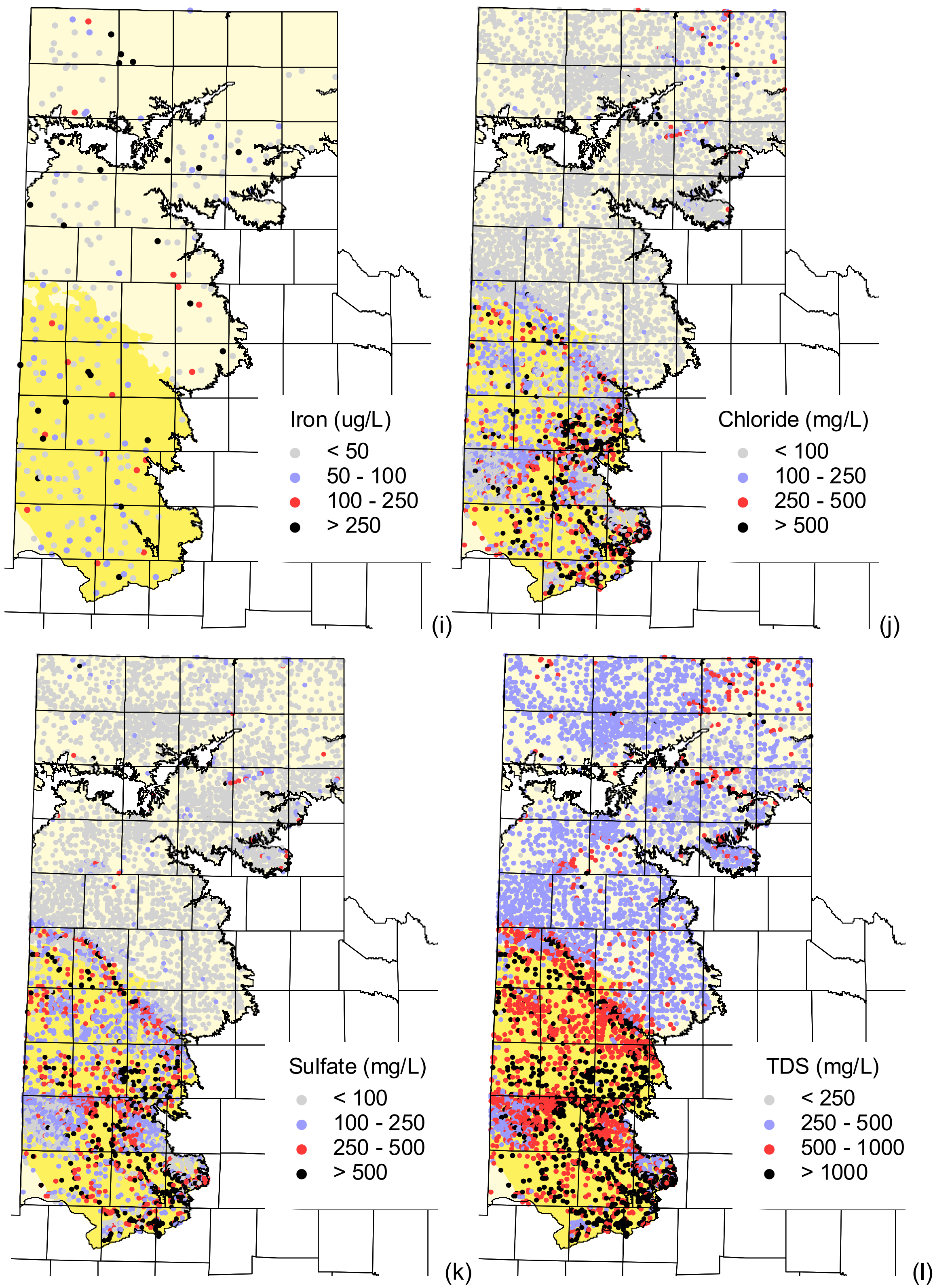

Figure 49. Spatial distribution of As (a), Mo (b), Se (c), V (d), B (e), F (f), U (g), silica (h), Fe (i), chloride (j), sulfate (k), TDS (l), and pH (m) in High Plains aquifers. All plots use only TWDB data except U where NURE data are used. (continued)

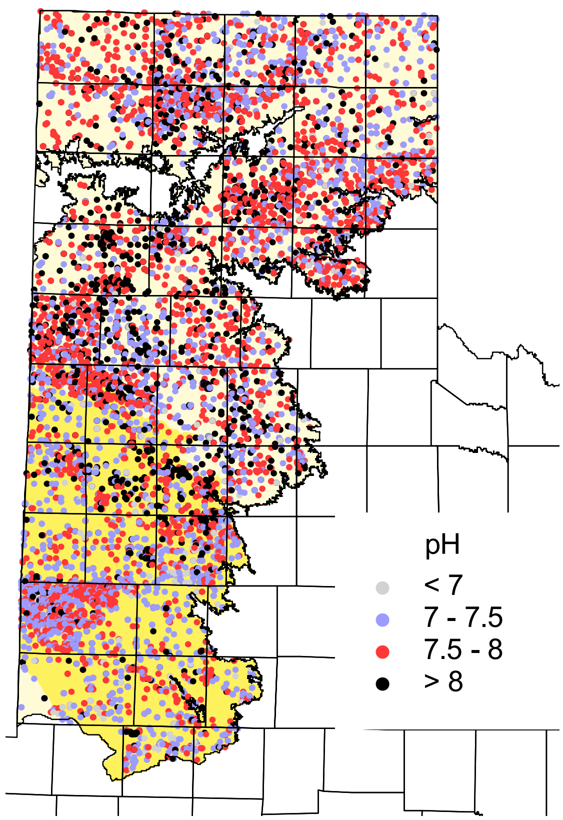

Figure 49. Spatial distribution of As (a), Mo (b), Se (c), V (d), B (e), F (f), U (g), silica (h), Fe (i), chloride (j), sulfate (k), TDS (l), and pH (m) in High Plains aquifers. All plots use only TWDB data except U where NURE data are used. (continued)

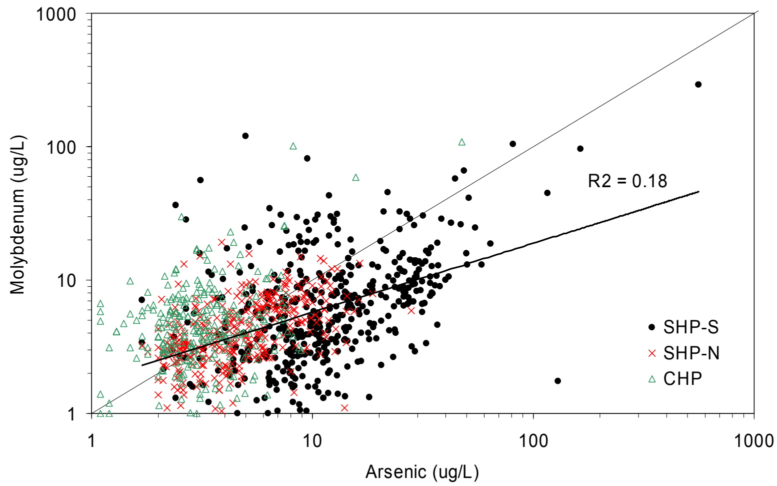

(a)

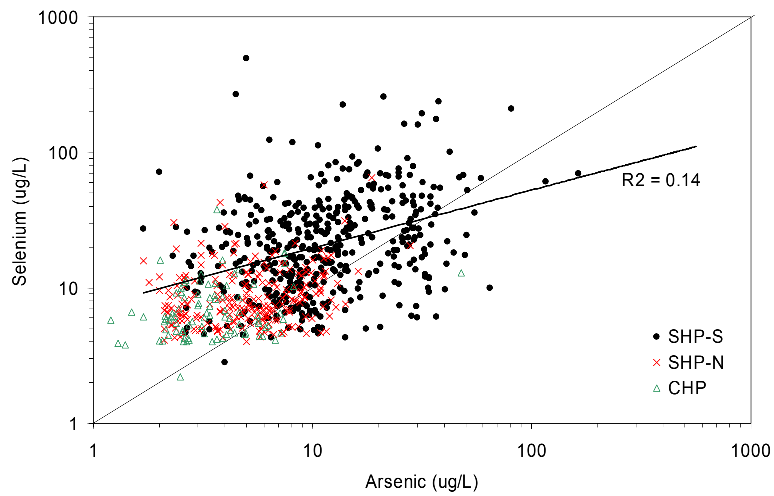

(b)

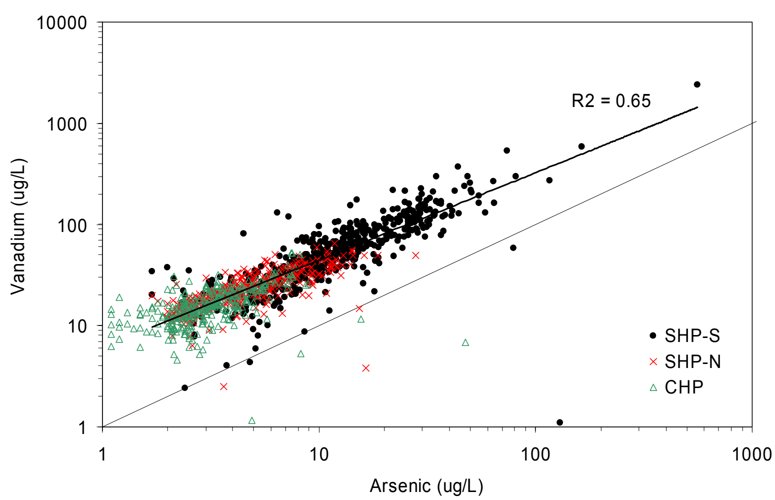

(c)

Figure 50. Cross-plots of (a) As vs. Mo, (b) vs. Se, (c) vs. V, (d) vs. B, (e) vs. F, (f) vs. silica, (g) vs. Fe, (h) vs. bicarbonate, (i) vs. sulfate, (j) vs. chloride, (l) vs. TDS and (m) vs. pH (NURE data set), High Plains aquifers.

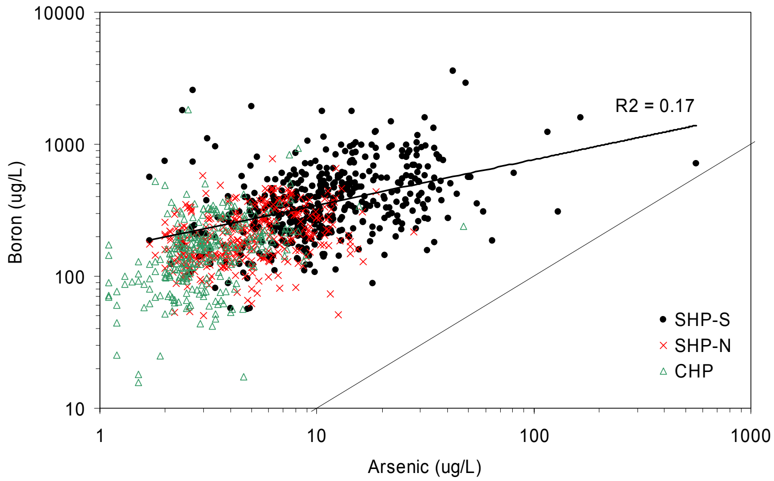

(d)

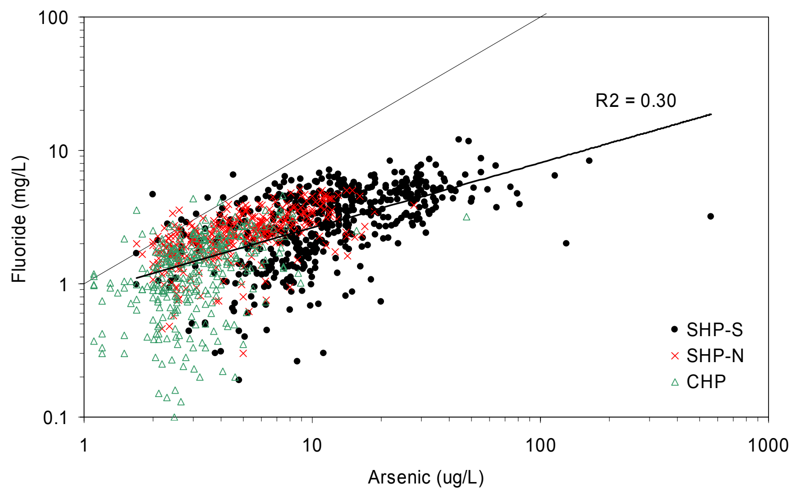

(e)

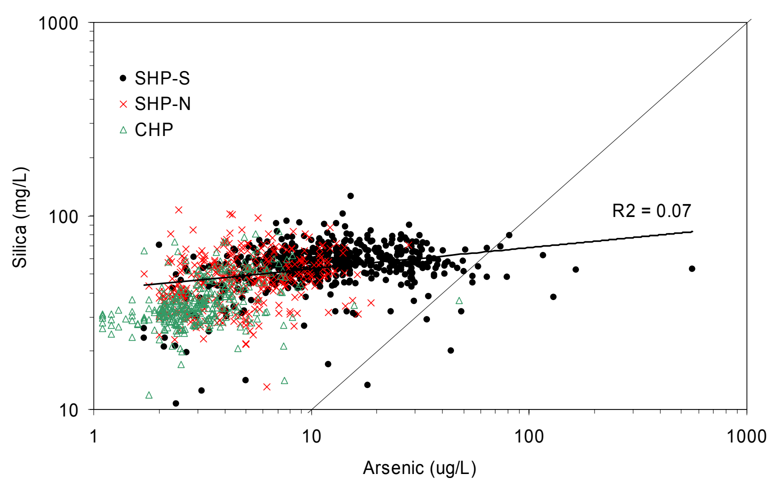

(f)

Figure 50. Cross-plots of (a) As vs. Mo, (b) vs. Se, (c) vs. V, (d) vs. B, (e) vs. F, (f) vs. silica, (g) vs. Fe, (h) vs. bicarbonate, (i) vs. sulfate, (j) vs. chloride, (l) vs. TDS and (m) vs. pH (NURE data set), High Plains aquifers. (continued)

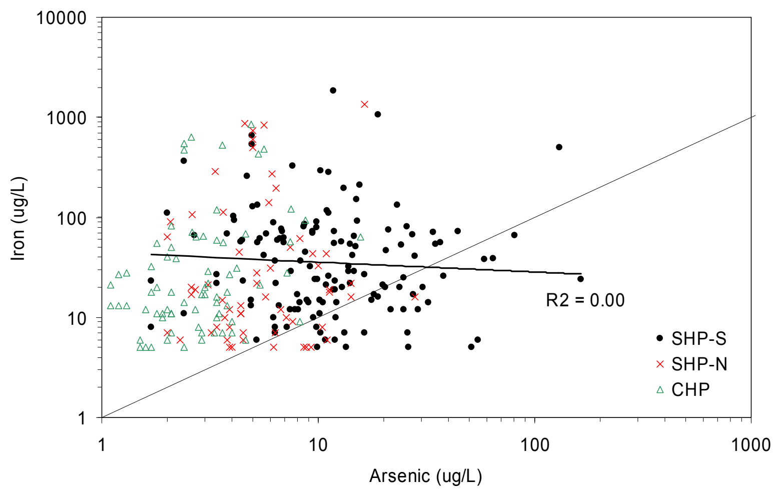

(g)

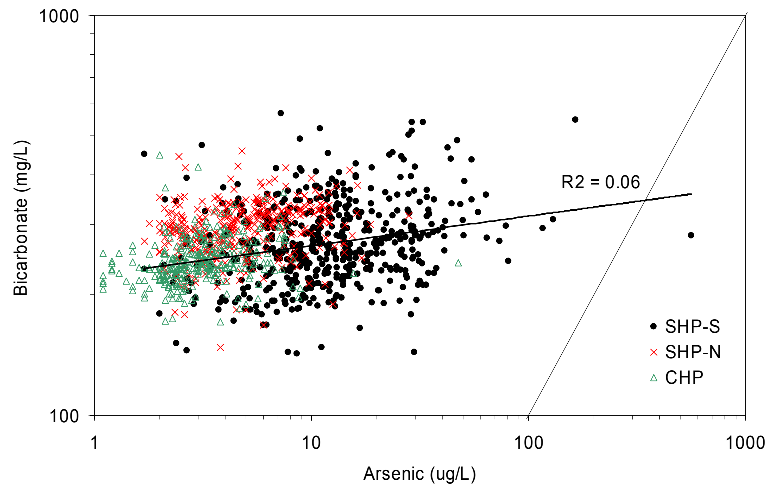

(h)

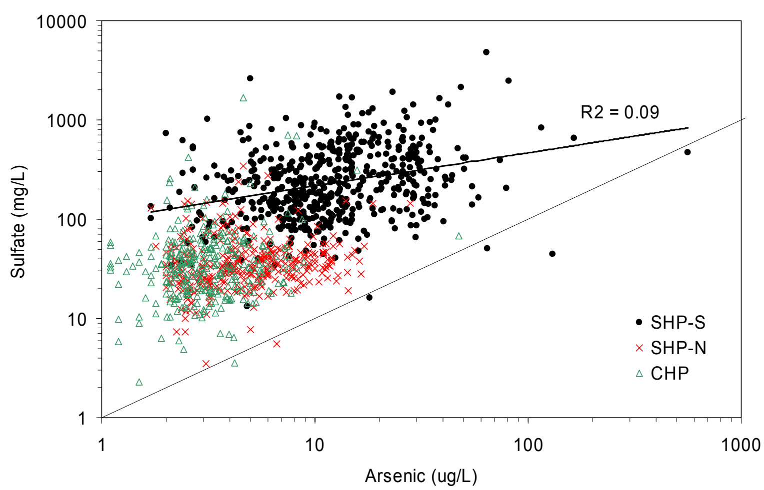

(i)

Figure 50. Cross-plots of (a) As vs. Mo, (b) vs. Se, (c) vs. V, (d) vs. B, (e) vs. F, (f) vs. silica, (g) vs. Fe, (h) vs. bicarbonate, (i) vs. sulfate, (j) vs. chloride, (l) vs. TDS and (m) vs. pH (NURE data set), High Plains aquifers. (continued)

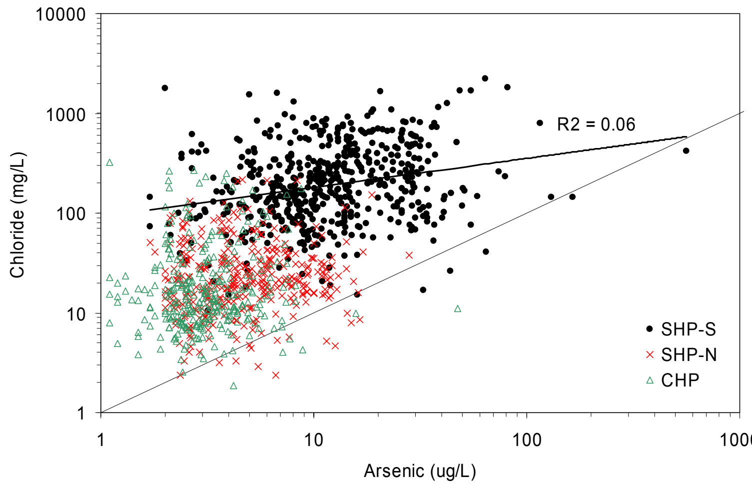

(j)

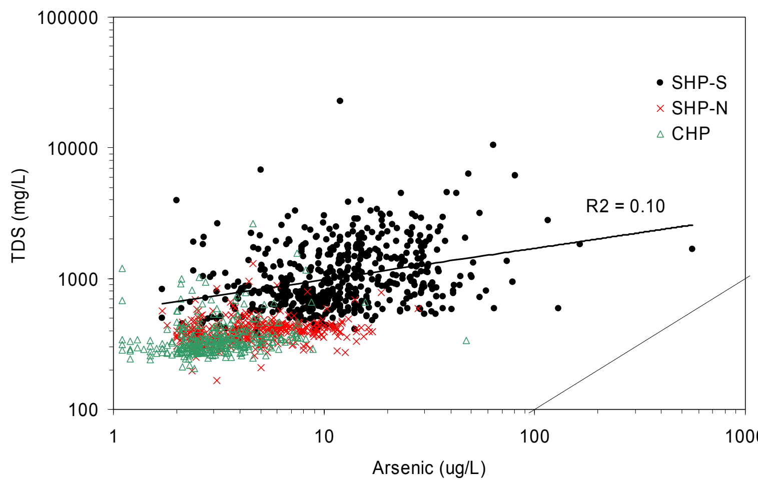

(l)

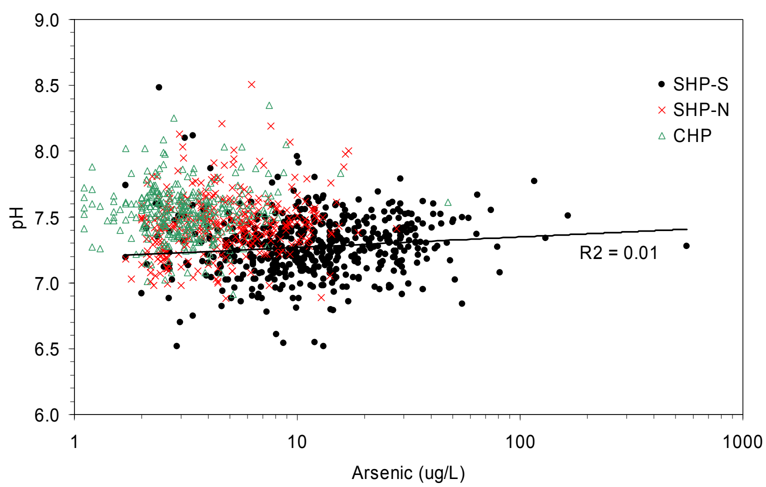

(m)

Figure 50. Cross-plots of (a) As vs. Mo, (b) vs. Se, (c) vs. V, (d) vs. B, (e) vs. F, (f) vs. silica, (g) vs. Fe, (h) vs. bicarbonate, (i) vs. sulfate, (j) vs. chloride, (l) vs. TDS and (m) vs. pH (NURE data set), High Plains aquifers. (continued)

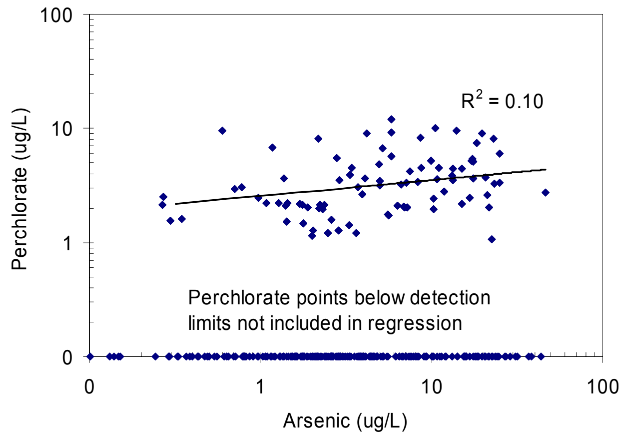

NOTE: Data set from Public Water Supply well sampling (Jackson et al., 2004)

Figure 51. Cross-plot of As vs. perchlorate, southern High Plain aquifers.

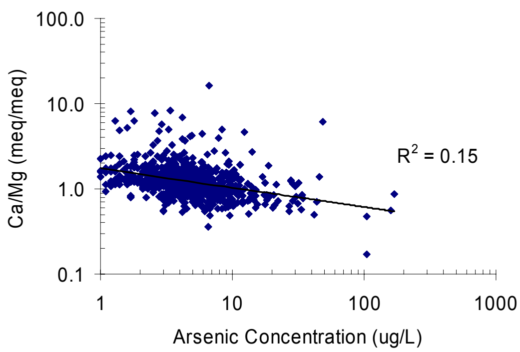

(a)

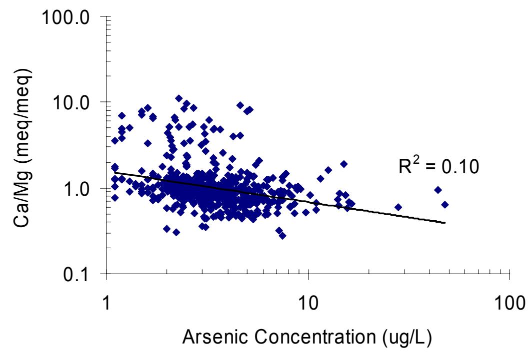

(b)

Figure 52. Cross-plot of As vs. Ca/Mg ratio, southern High Plains; NURE (a) and TWDB (b) databases

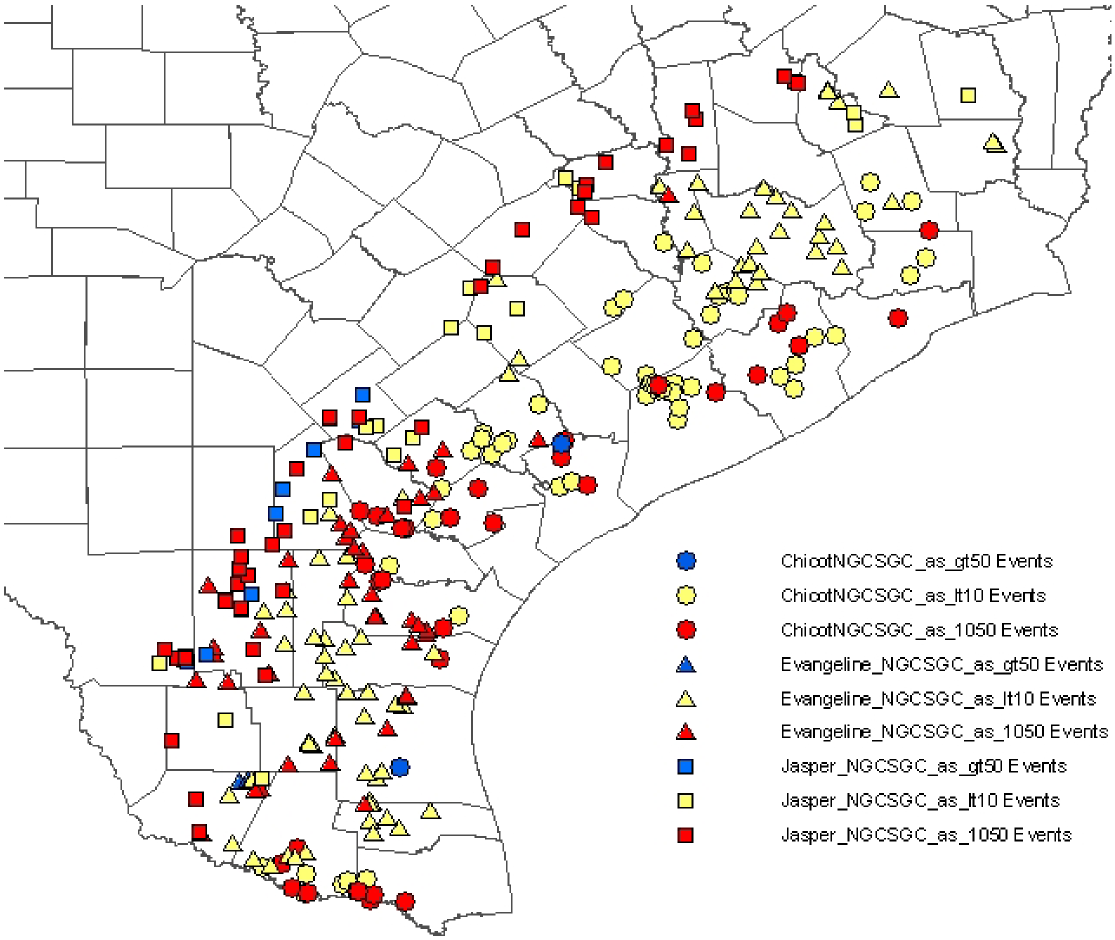

(a)

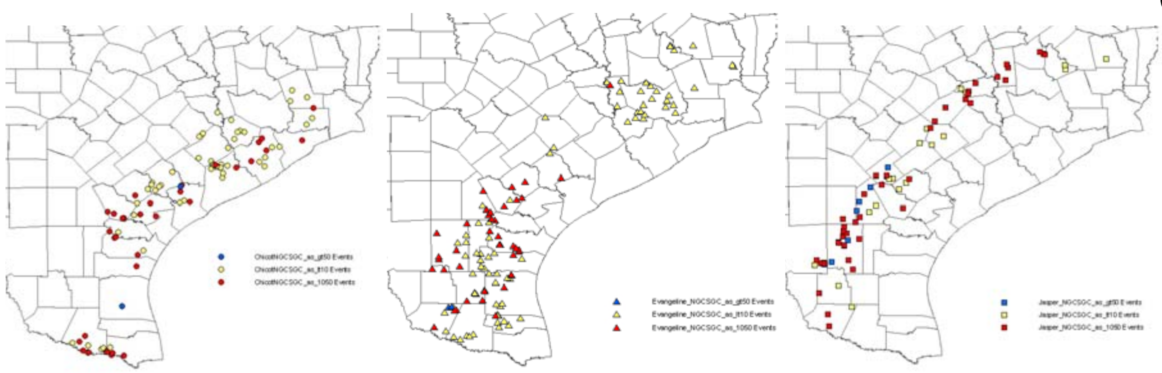

(b)

Figure 53. Arsenic spatial distribution by aquifer: all together (a) and, individually, in Chicot, Evangeline, and Jasper aquifers (b).

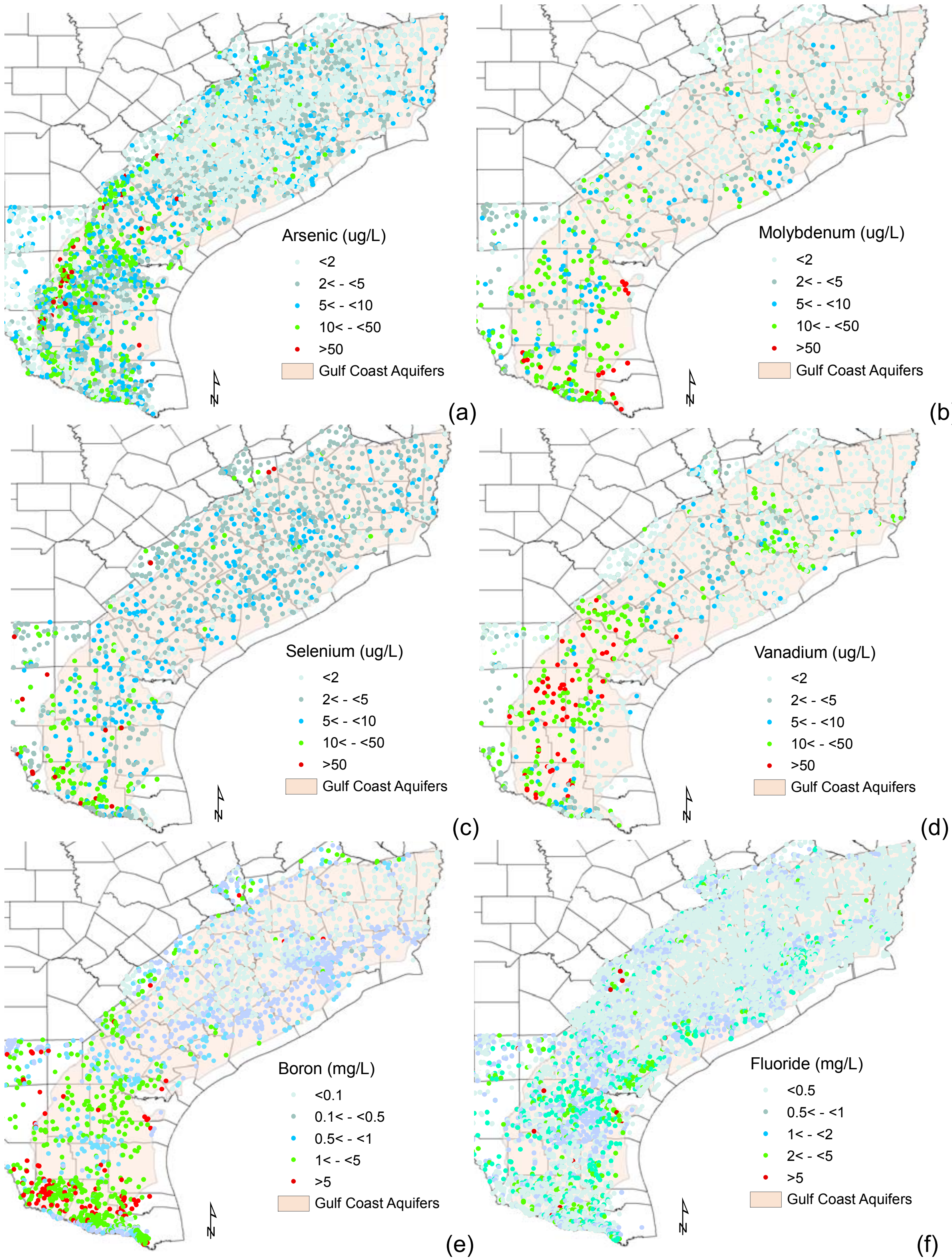

Figure 54. Spatial distribution of As (a), Mo (b), Se (c), V (d), B (e), F (f), U (g), silica (h), Fe (i), chloride (j), sulfate (k), TDS (l), anf pH (m) in Gulf Coast aquifers. All plots use only TWDB data except As and U where NURE data are also included.

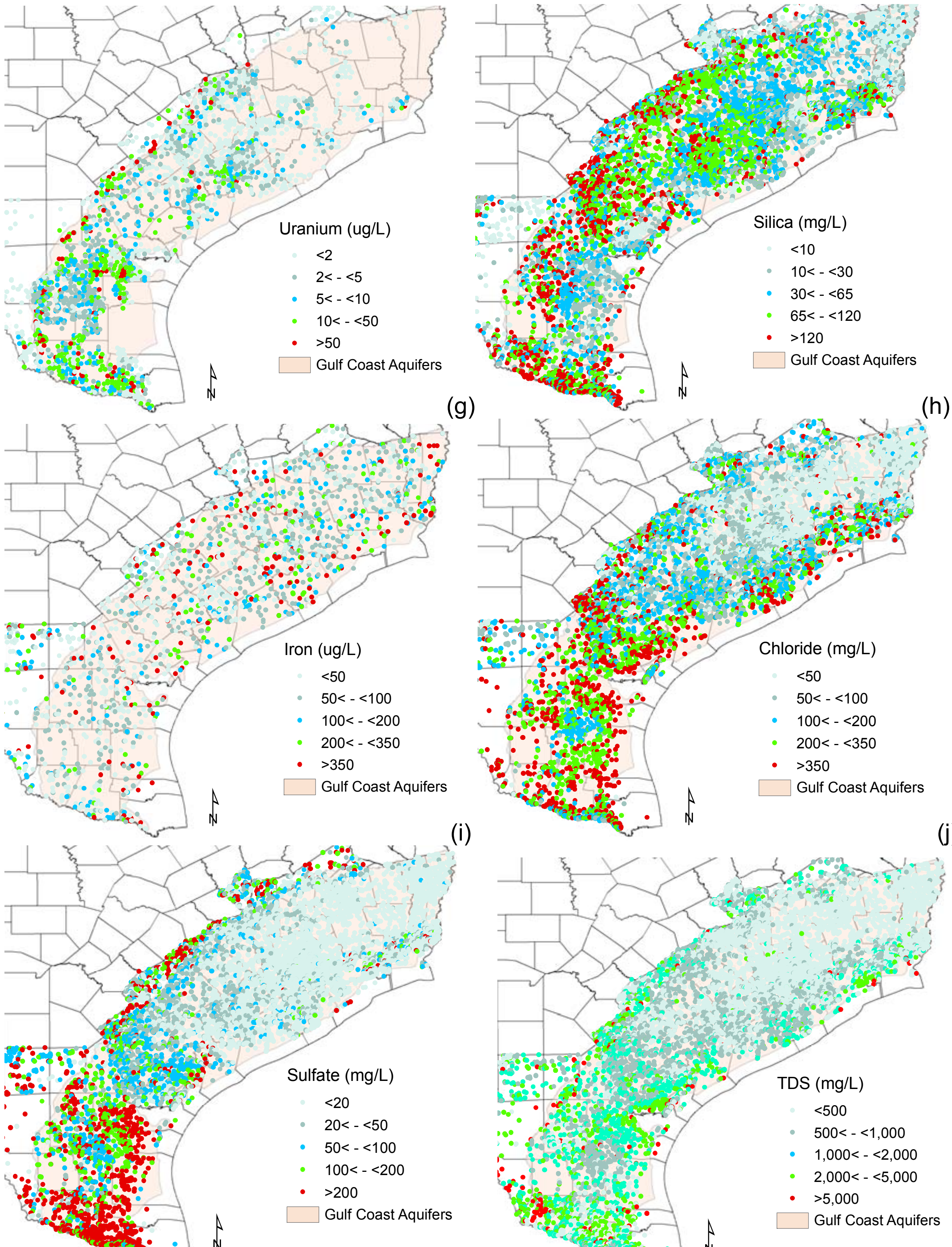

Figure 54. Spatial distribution of As (a), Mo (b), Se (c), V (d), B (e), F (f), U (g), silica (h), Fe (i), chloride (j), sulfate (k), TDS (l), anf pH (m) in Gulf Coast aquifers. All plots use only TWDB data except As and U where NURE data are also included. (continued)

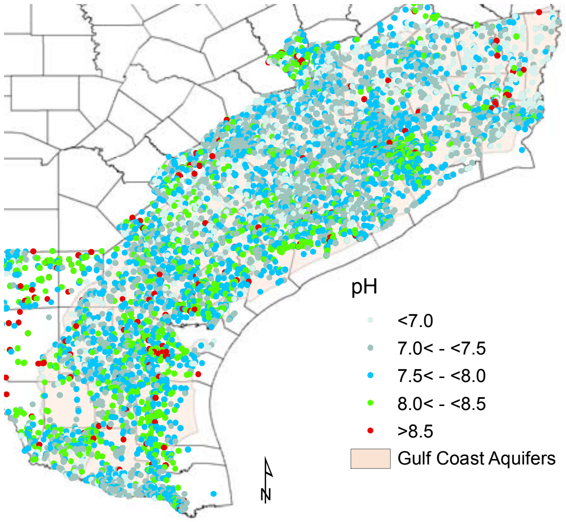

(m)

Figure 54. Spatial distribution of As (a), Mo (b), Se (c), V (d), B (e), F (f), U (g), silica (h), Fe (i), chloride (j), sulfate (k), TDS (l), anf pH (m) in Gulf Coast aquifers. All plots use only TWDB data except As and U where NURE data are also included. (continued)

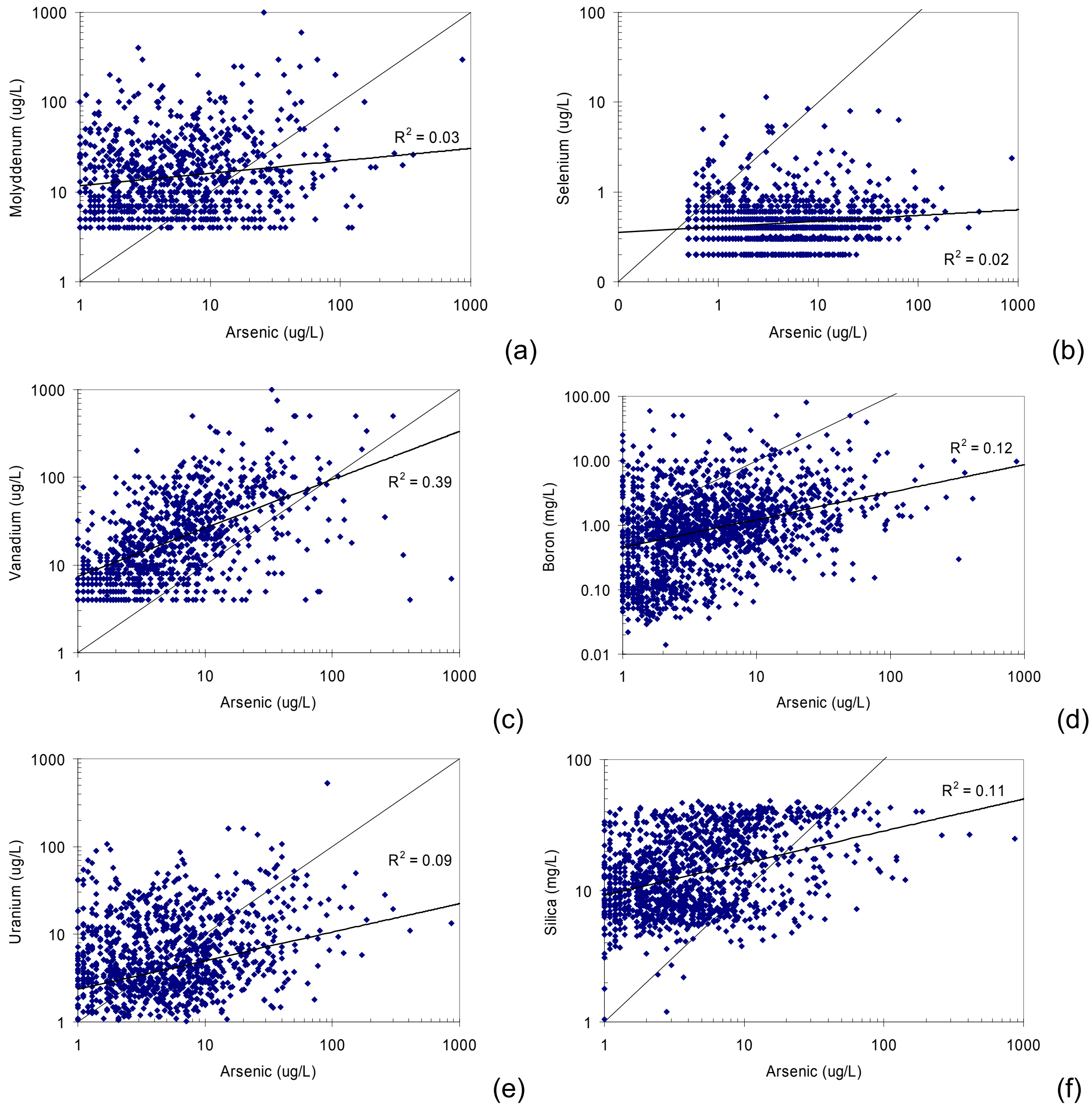

Figure 55. Cross-plots of (a) As vs. Mo, (b) vs. Se, (c) vs. V, (d) vs. B, (e) vs. U, (f) vs. silica, (g) vs. Fe, (h) vs. alkalinity (~bicarbonate), (i) sulfate, (j) vs. chloride, (k) vs. conductivity (~TDS) and (l) vs. pH (NURE data set), southwestern Gulf Coast aquifers.

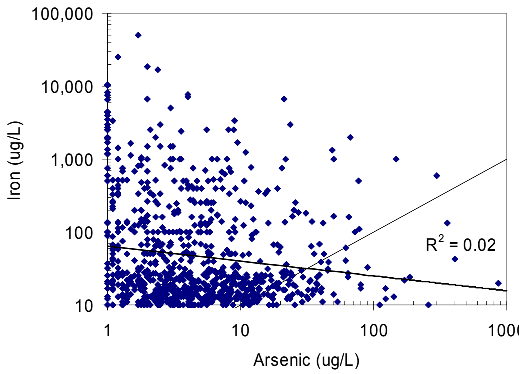

(g)

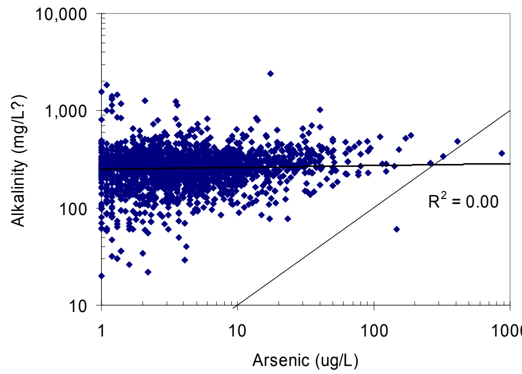

(h)

NOTE: Reporting unit was not given (mg/L?)

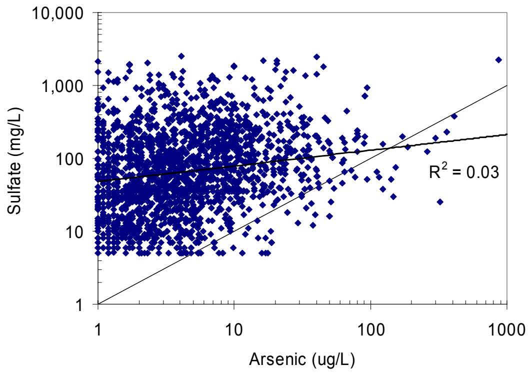

(i)

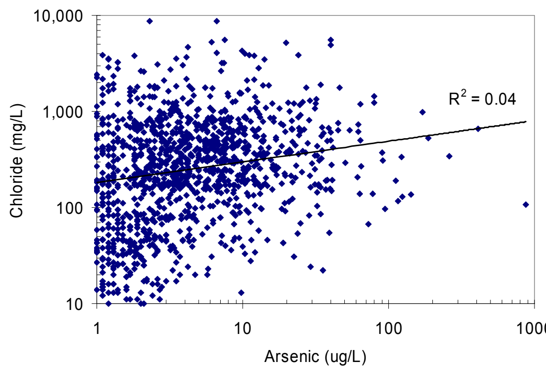

(j)

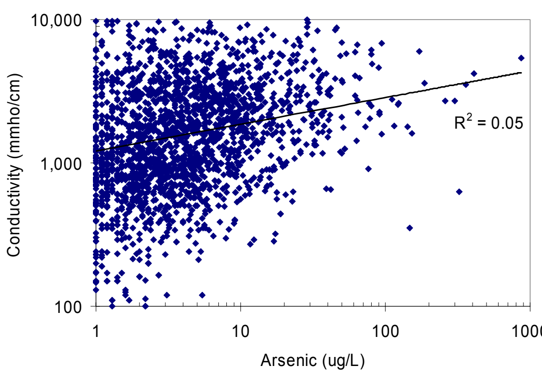

(k)

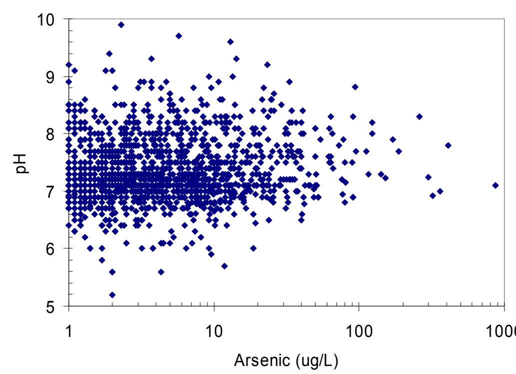

(l)

Figure 55. Cross-plots of (a) As vs. Mo, (b) vs. Se, (c) vs. V, (d) vs. B, (e) vs. U, (f) vs. silica, (g) vs. Fe, (h) vs. alkalinity (~bicarbonate), (i) sulfate, (j) vs. chloride, (k) vs. conductivity (~TDS) and (l) vs. pH (NURE data set), southwestern Gulf Coast aquifers. (continued)

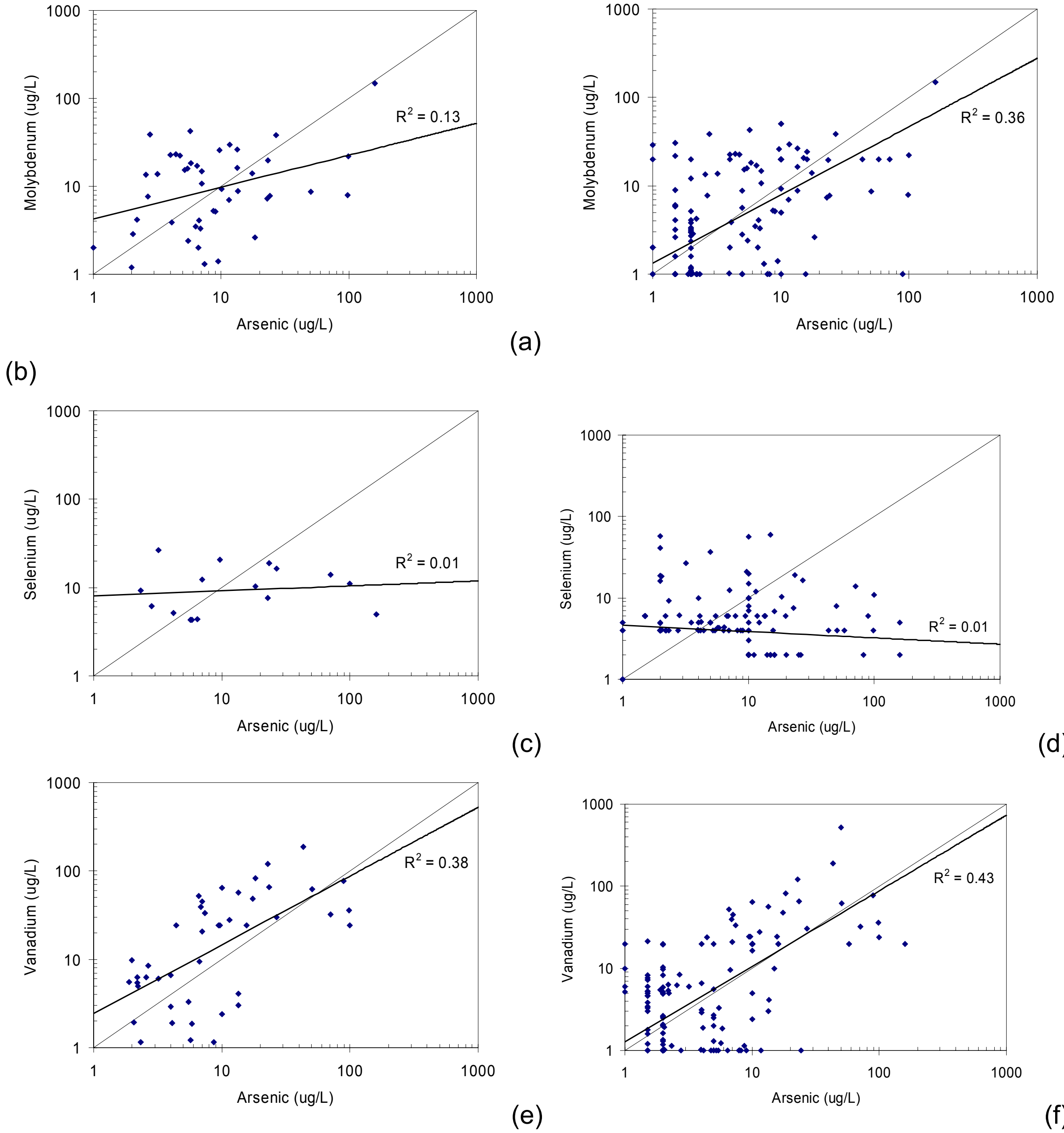

NOTE: Left-hand side plots include only those sample points where both variables are above detection limits; right-hand side plots include all sample points

Figure 56. Cross-plots of (a,b) As vs. Mo, (c,d) vs. Se, (e,f) vs. V, (g,h) vs. B, (i) vs. fluoride and silica, (j) vs. bicarbonate and sulfate, (k) vs. nitrate, and (l) vs. TDS and pH (TWDB database), southwestern Gulf Coast aquifers.

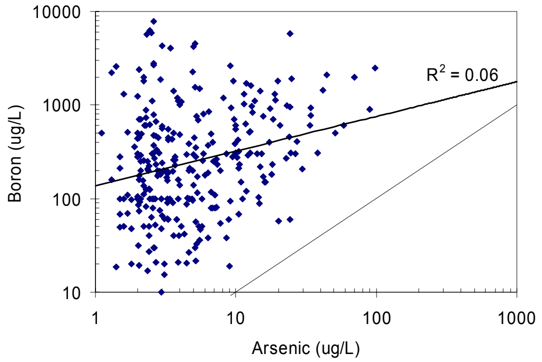

(g)

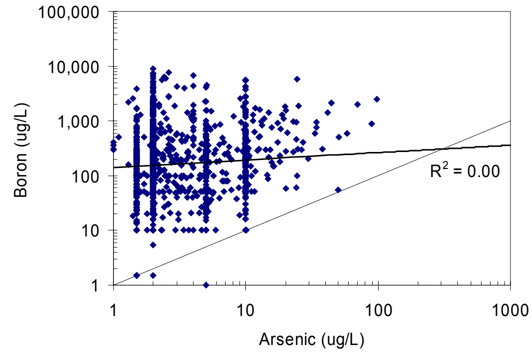

(h)

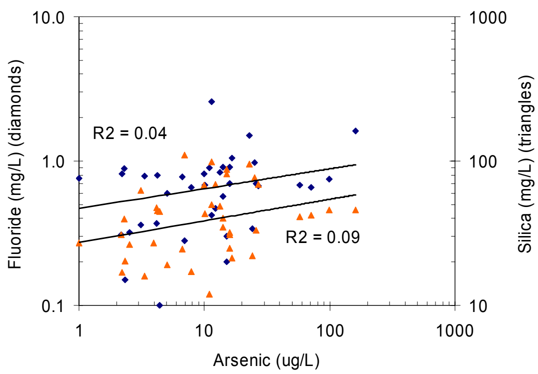

(i)

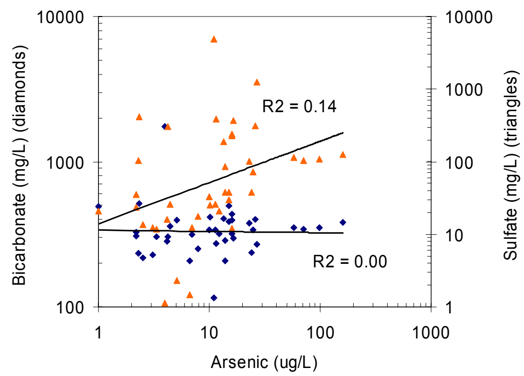

(j)

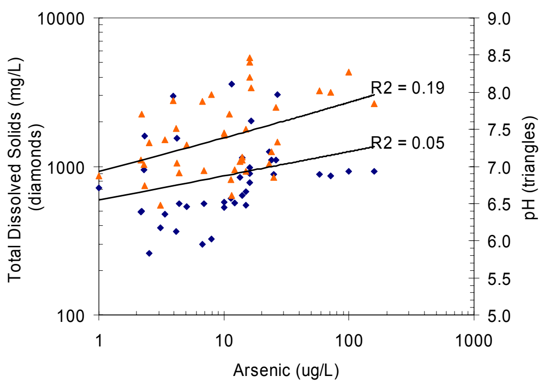

(k)

NOTE: all plots include only those sample points where both variables are above detection limits except (h) that include all sample points.

Figure 56. Cross-plots of (a,b) As vs. Mo, (c,d) vs. Se, (e,f) vs. V, (g,h) vs. B, (i) vs. fluoride and silica, (j) vs. bicarbonate and sulfate, (k) vs. nitrate, and (l) vs. TDS and pH (TWDB database), southwestern Gulf Coast aquifers. (continued)

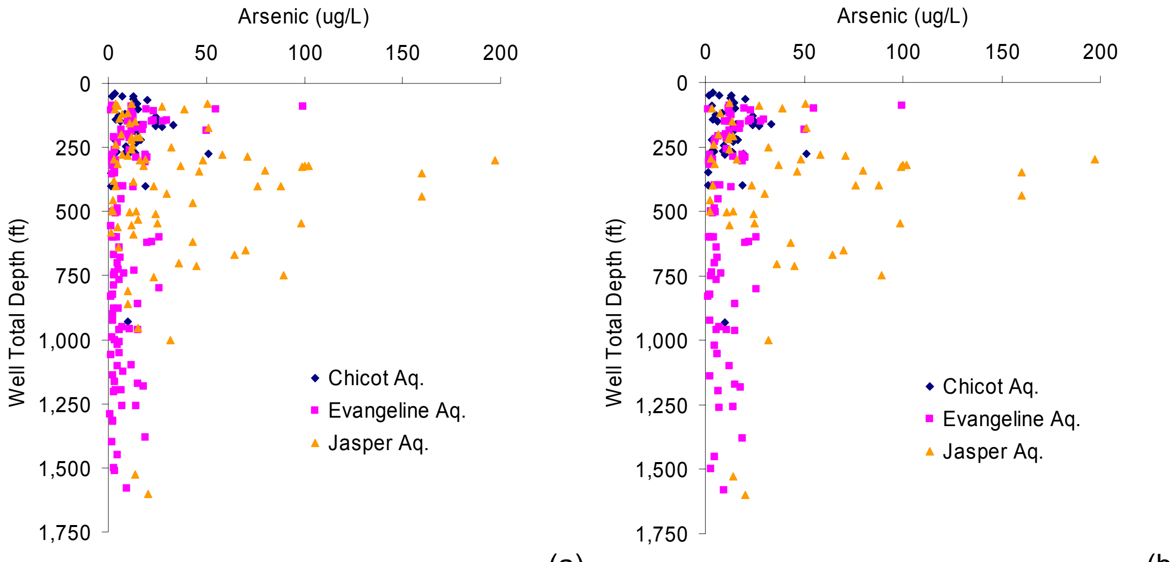

Figure 57. Arsenic concentration vs. total well depth in Gulf Coast Aquifers (a), only southwestern Gulf Coast (b)

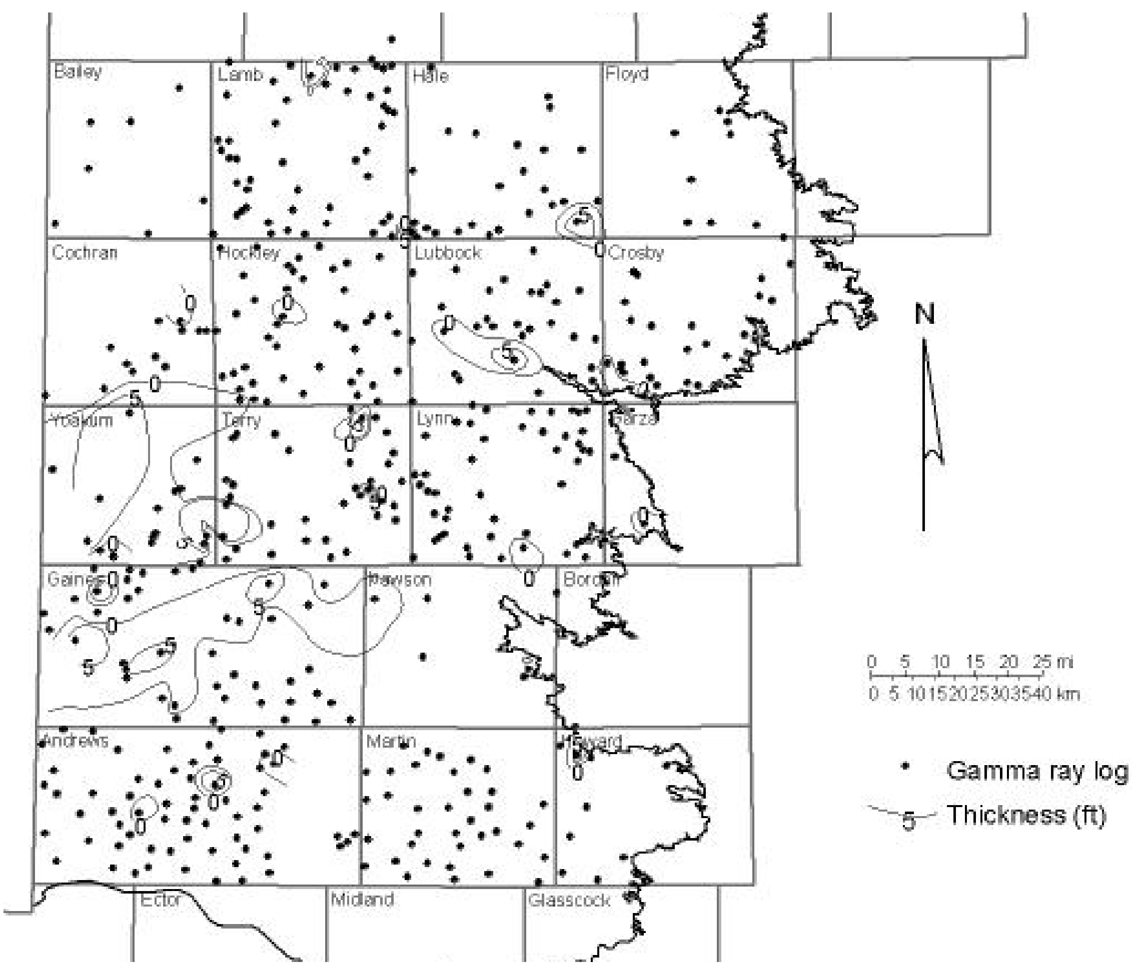

Figure 58. Thickness map of Ogallala-age ash beds based on geophysical logs

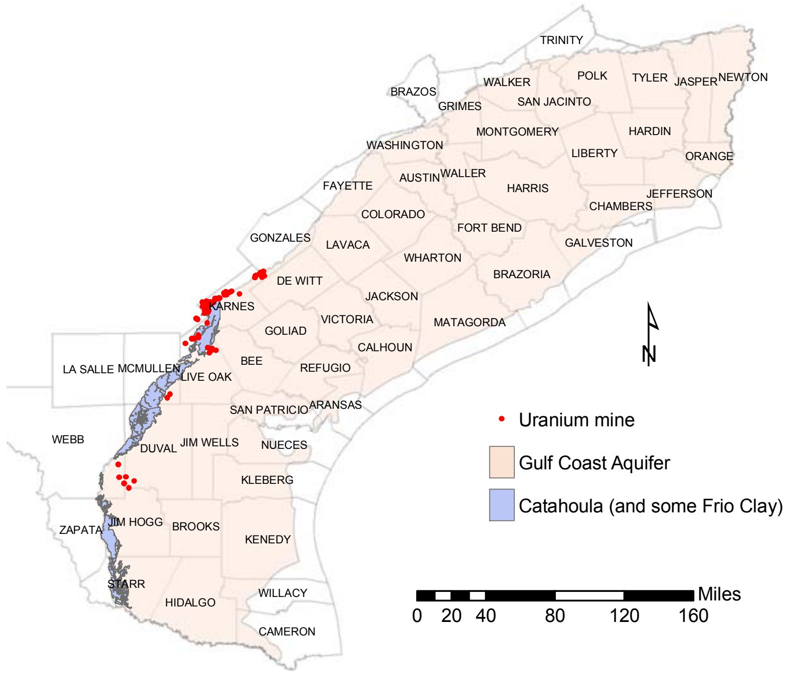

Figure 59. Map of selected uranium mines in the southern Gulf Coast area

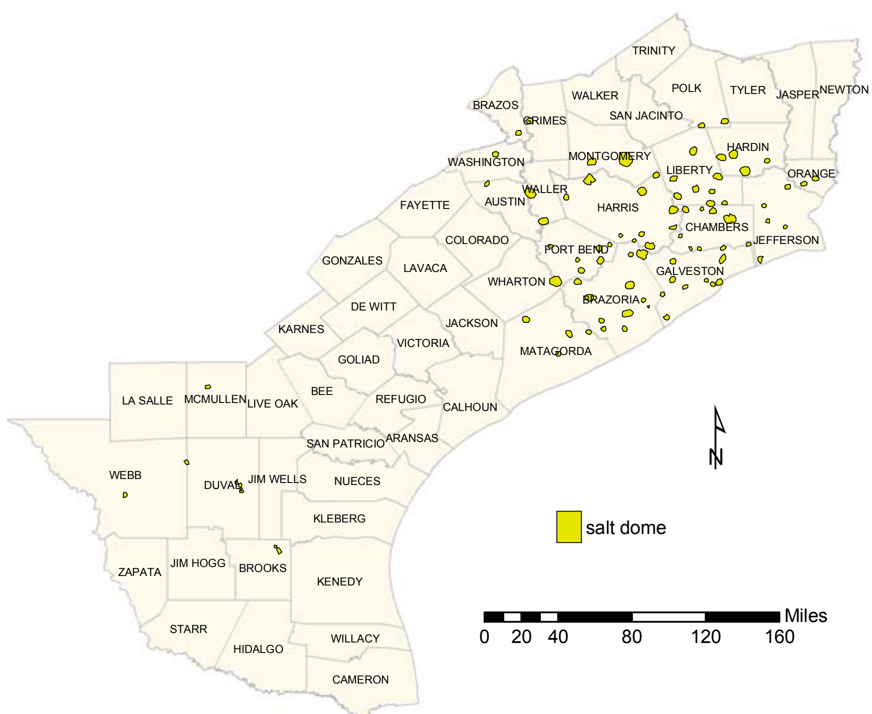

NOTE: locations from Lopez (1995), depth information from Halbouty (1979) and Ewing (1990)
Figure 60. Map of salt domes along the Gulf Coast

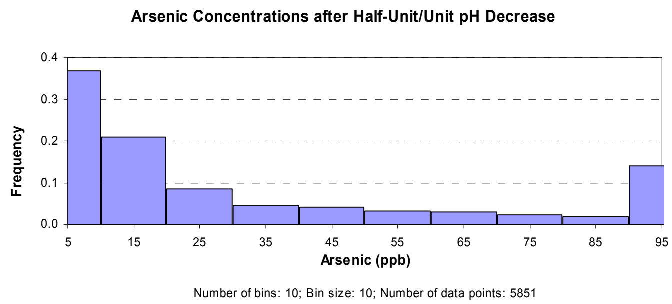

(a)

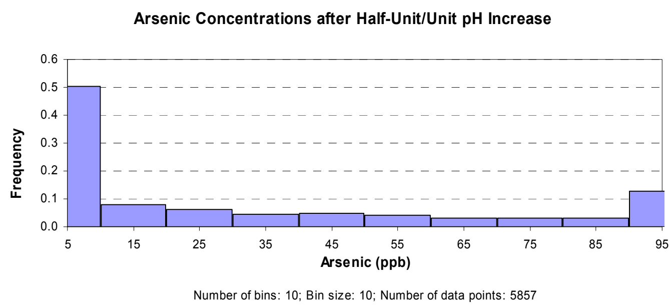

(b)

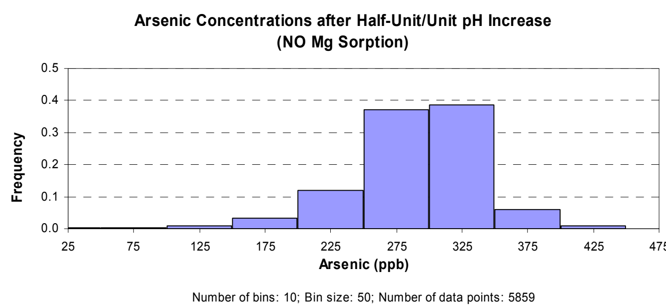

(c)

Figure 61. Histograms of arsenic distribution showing modeling results

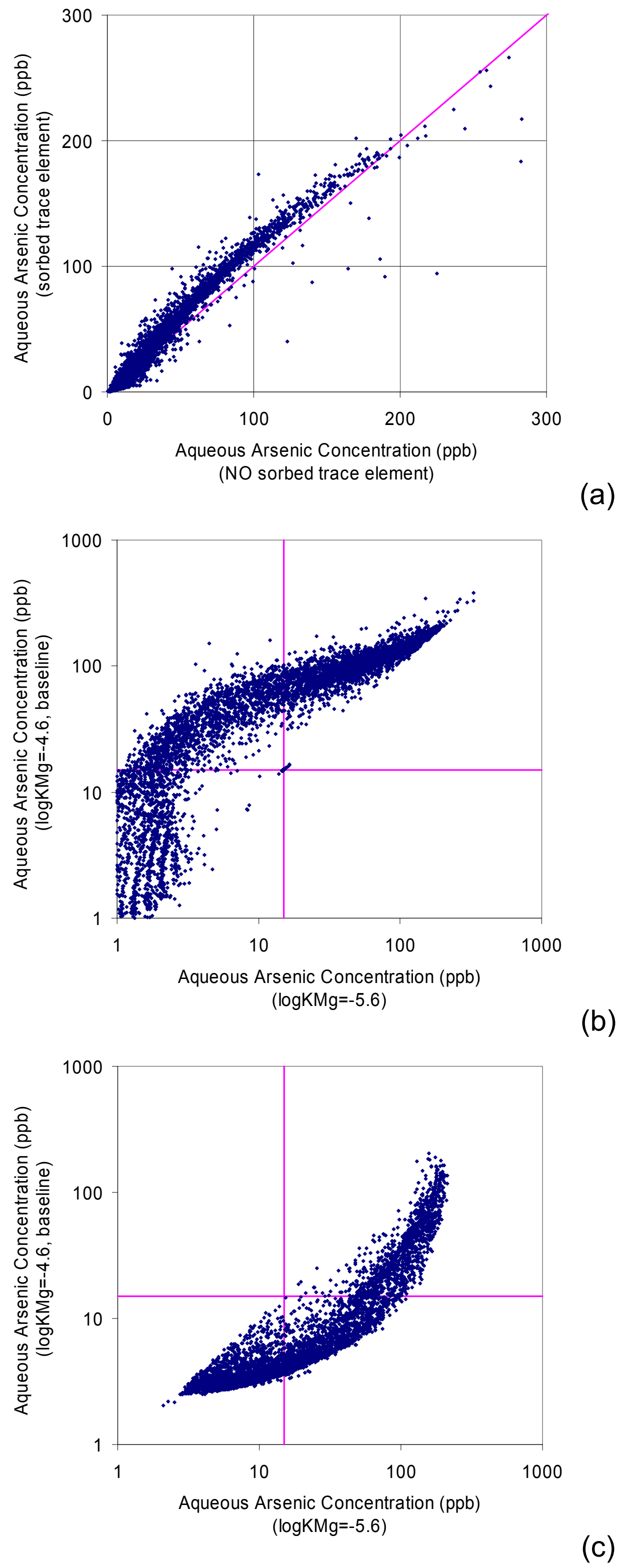

Figure 62. Crossplot of arsenic concentration with and without including trace elements in the modeling

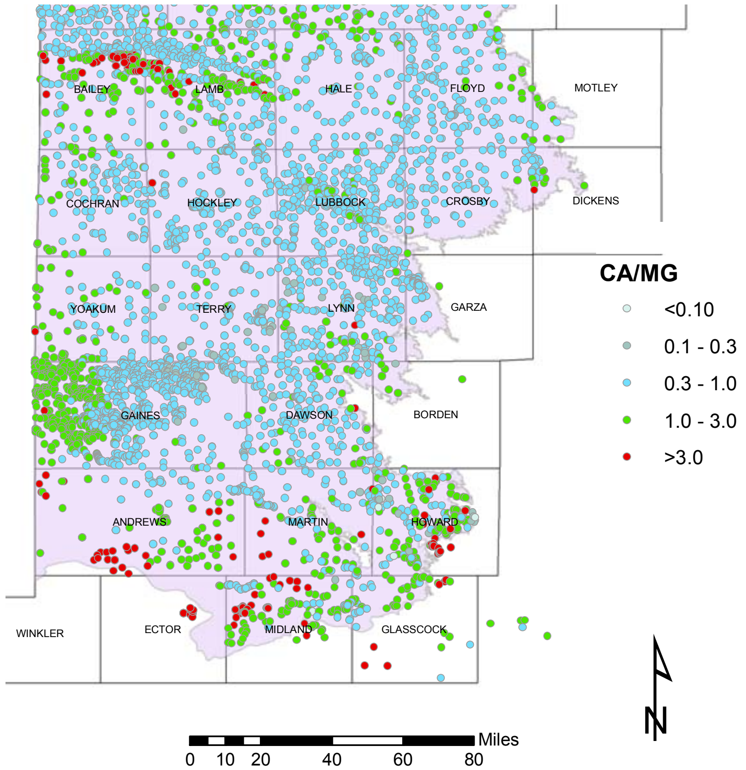

Figure 63. Spatial distribution of the Ca/Mg ratio in the southern High Plains (TWDB database)

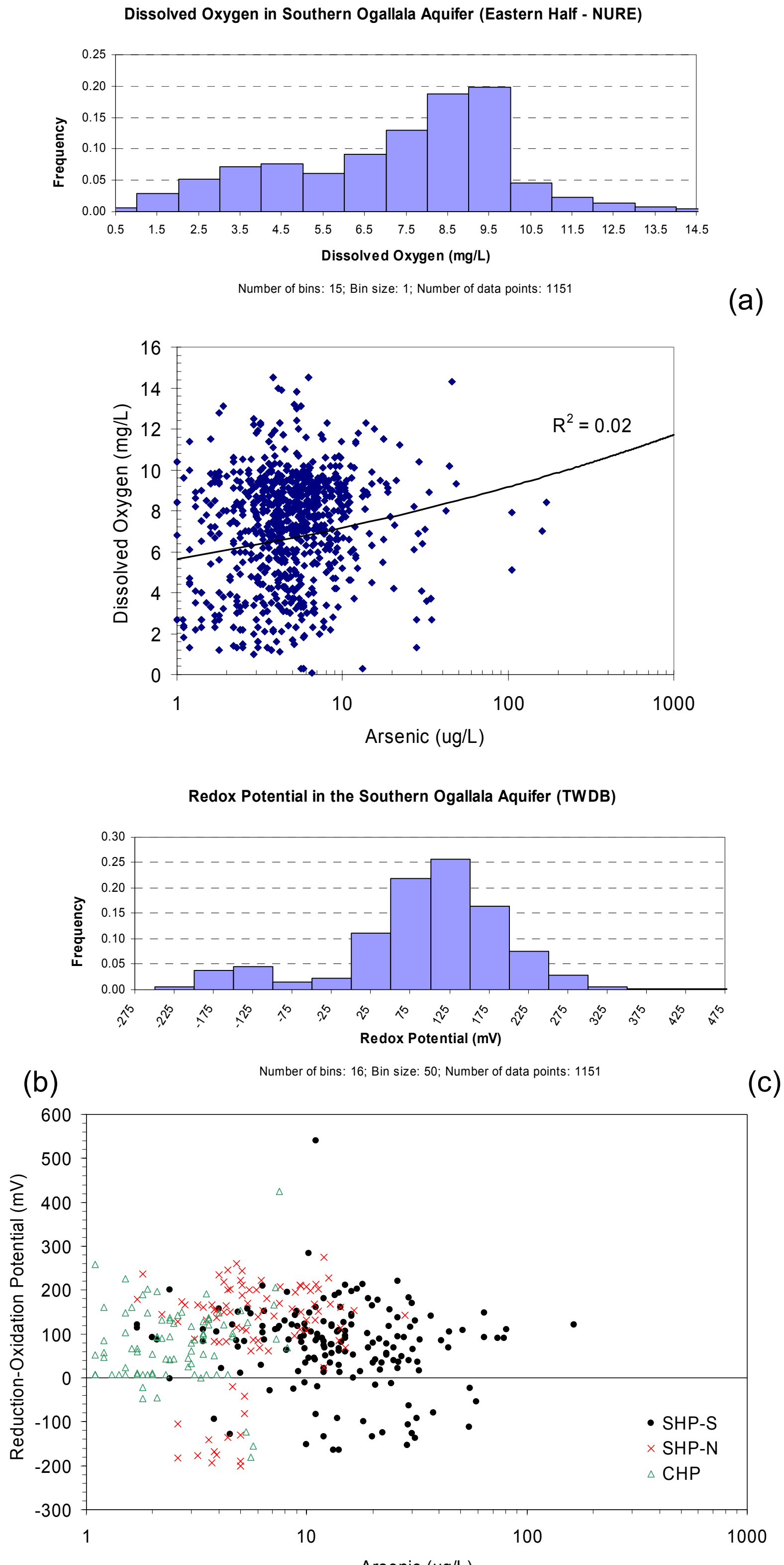

Figure 64. Distribution of dissolved oxygen (NURE) and redox potential (TWDB) in the southern High Plains aquifer

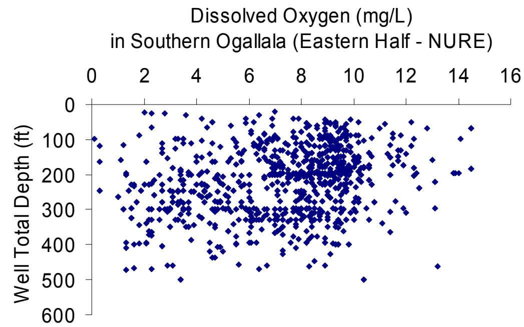

Figure 65. Depth distribution of dissolved oxygen in the eastern half of the southern High Plains aquifer (NURE data)

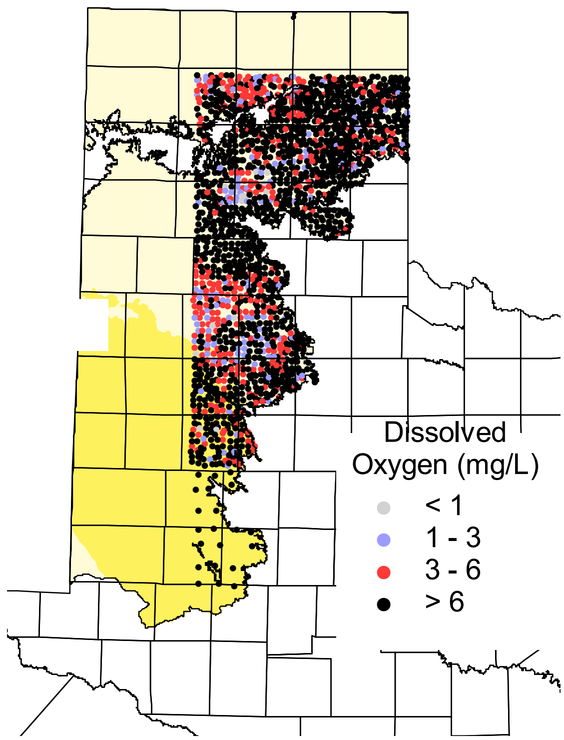

Figure 66. Spatial distribution of dissolved oxygen in the eastern half of the southern High Plains aquifer (NURE data)

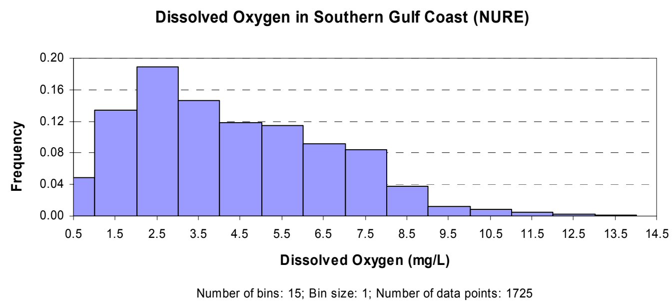

Figure 67. Histogram of dissolved oxygen in the southwestern Gulf Coast aquifers (NURE data)

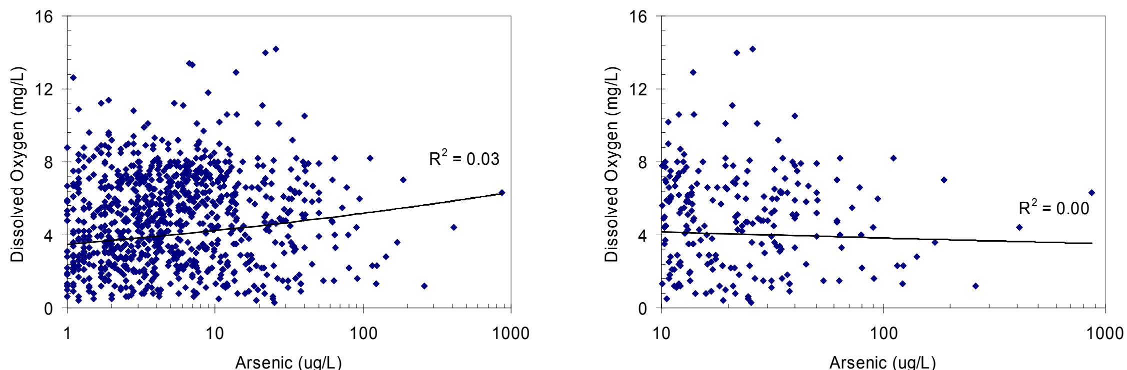

(a) (b)

NOTE: (a) all samples; (b) only samples with As > 10 ug /L are retained
Figure 68. Cross-plots of As vs. dissolved oxygen (NURE data set), southwestern Gulf Coast aquifers:

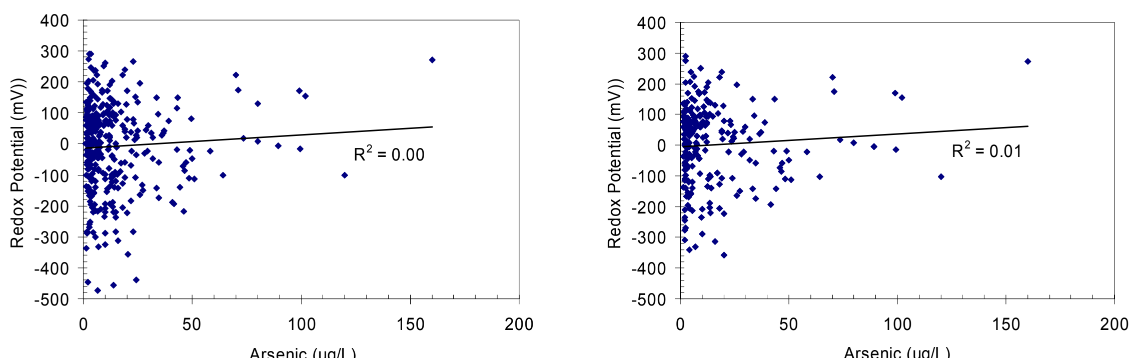

(a) (b)

Figure 69. Redox potential in Gulf Coast aquifers (a) and only southwestern section (b)

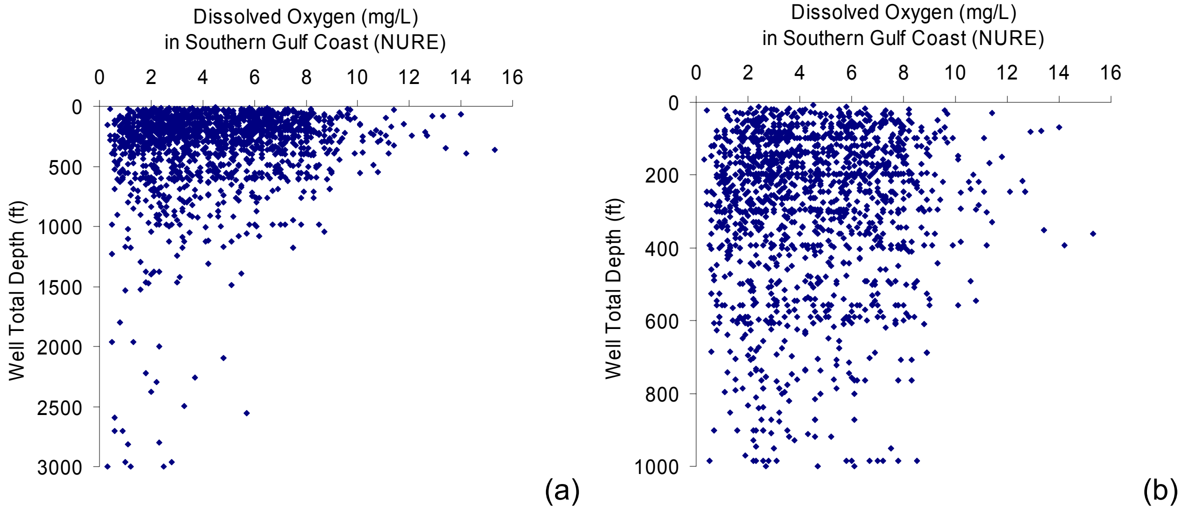

NOTE: (a) to a depth of 3,000 ft; (b) to a depth of 1,000 ft

Figure 70. Depth distribution of dissolved oxygen in the southwestern Gulf Coast aquifers

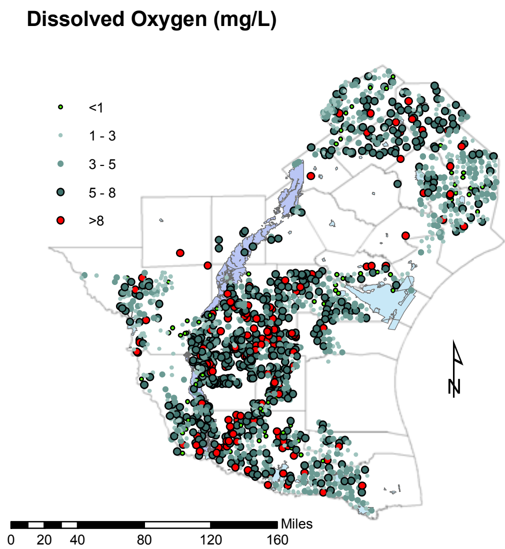

Figure 71. Spatial distribution of dissolved oxygen in the southwestern Gulf Coast aquifers (NURE)

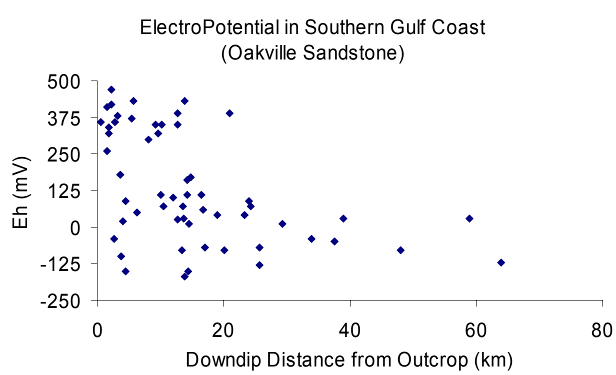

NOTE: data from Henry et al. (1982a, Table A-1)

Figure 72. Eh evolution along groundwater flowlines in Oakville sandstone of the southwestern Gulf Coast

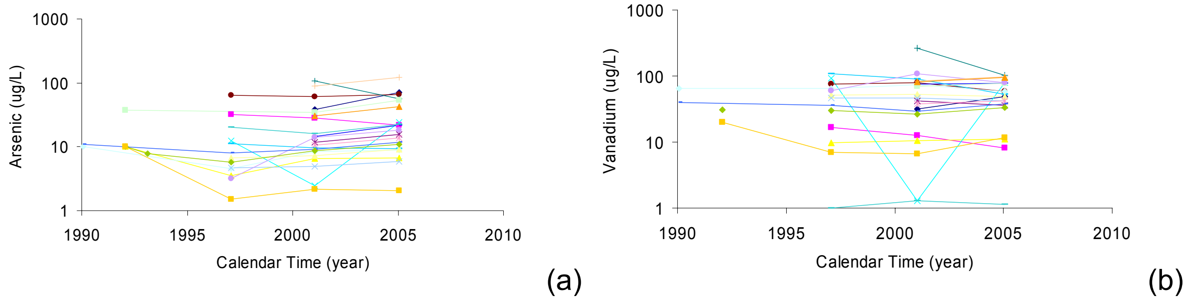

Figure 73. Time series of arsenic and Vanadium aqueous concentrations in wells recently sampled in Duval County

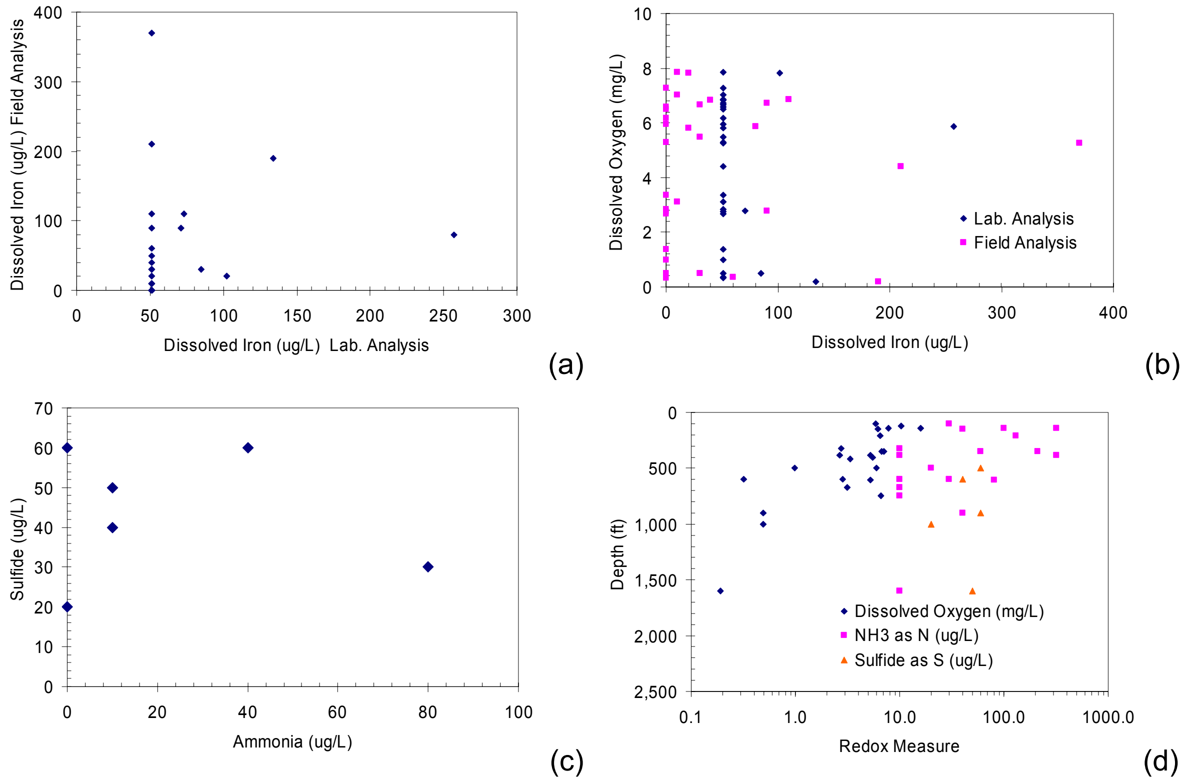

Figure 74. Analysis of redox pairs (Duval County)

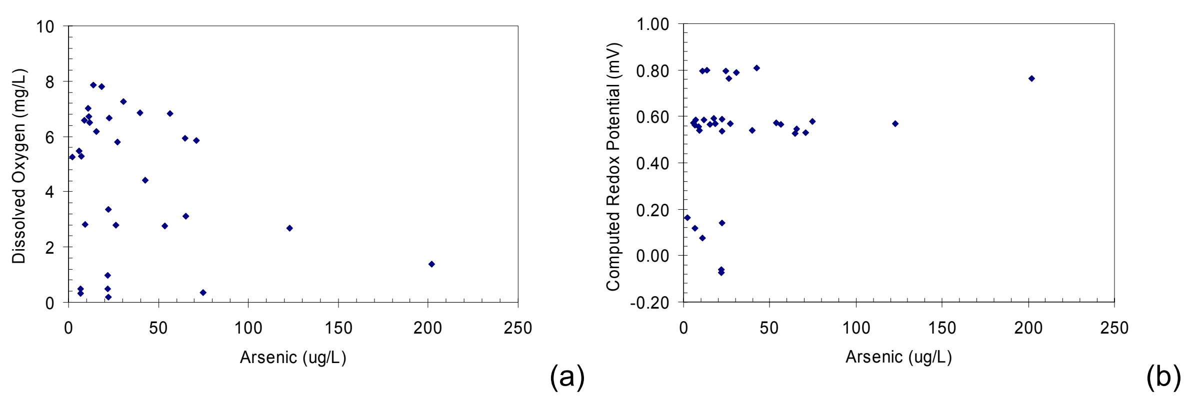

Figure 75. Cross-plots of As vs. dissolved oxygen (a) and computed redox potential (b) (Duval County)

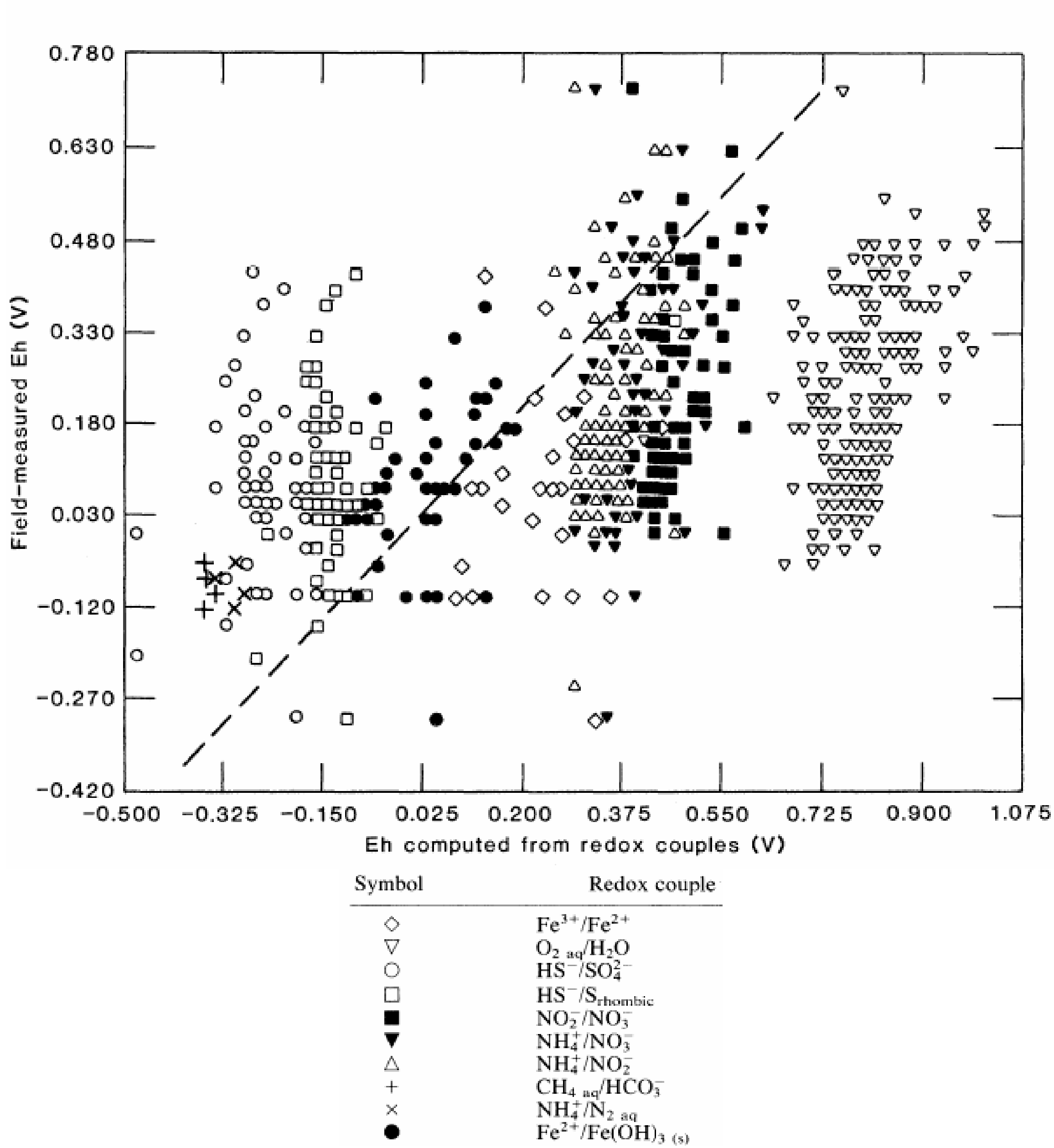

SOURCE: Lindberg and Runnels, 1994

Figure 76. Literature comparison of measured and computed Eh

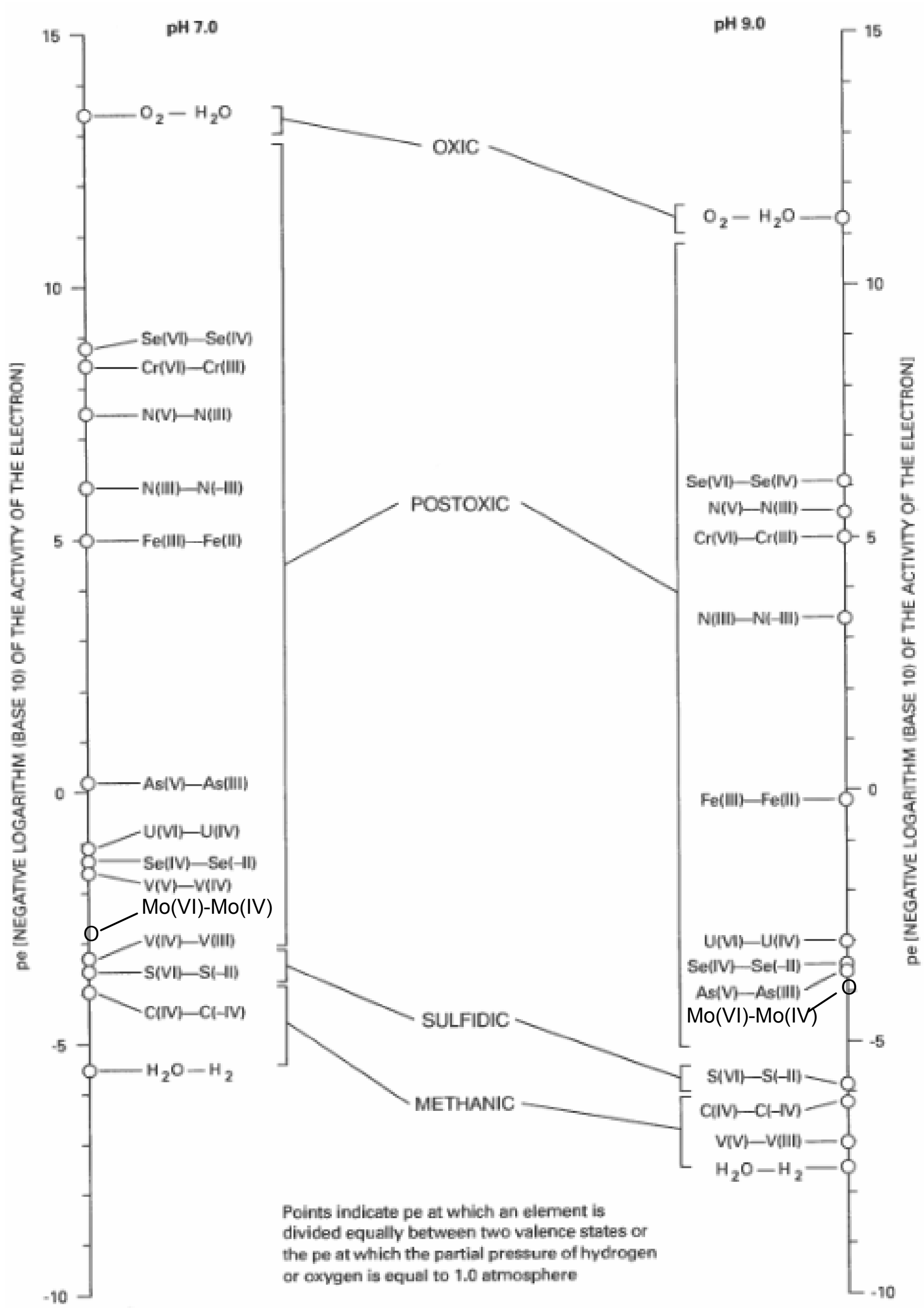

NOTE: at 25^{o}C, pe = 16.9 Eh (V) or Eh (mV) = 59 pe
SOURCE: Parkhurst et al., 1995
Figure 77. Redox ladder for As, Se, U, and V and major redox couples

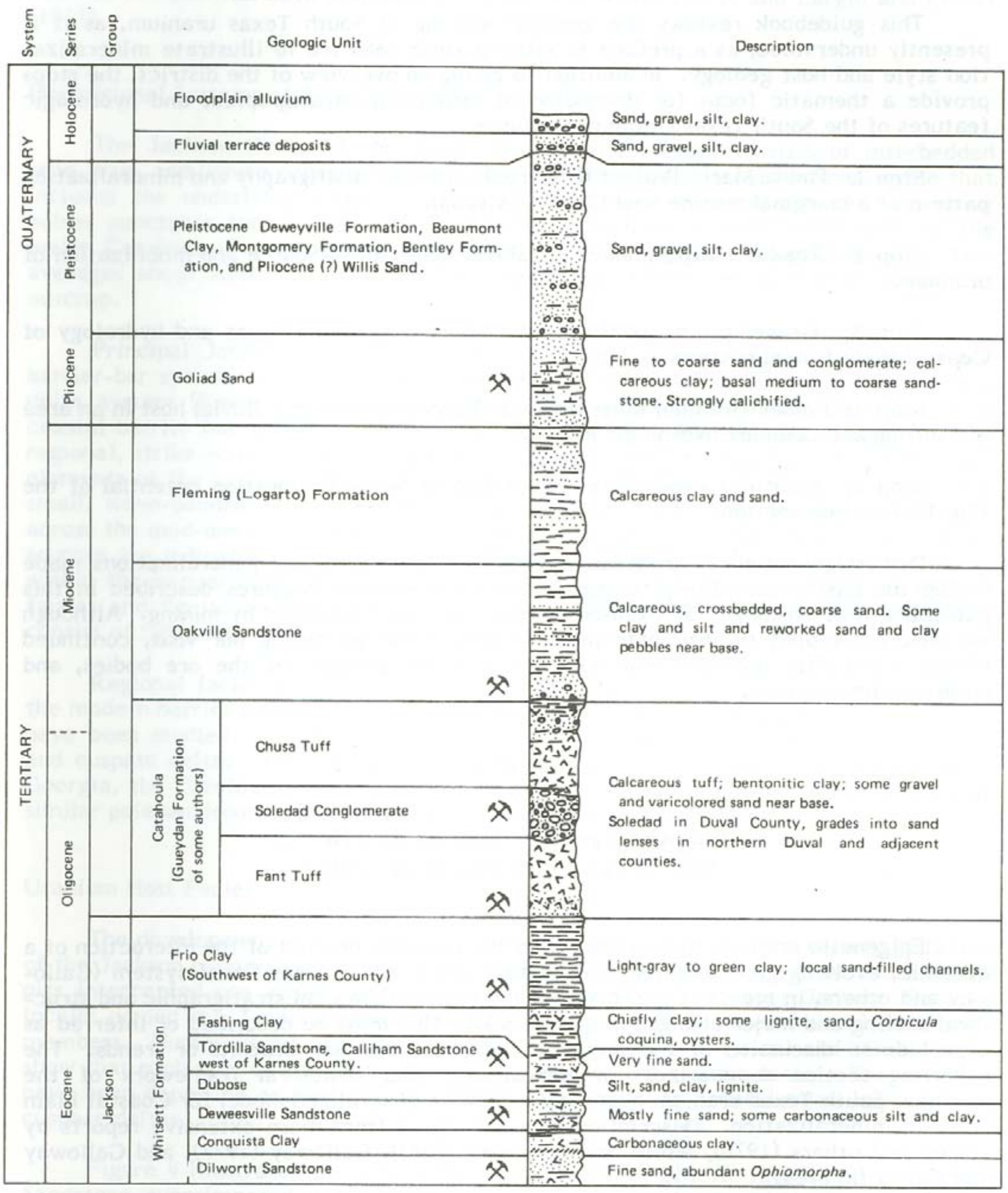

NOTE: Crossed picks indicate units from which uranium has been extracted
SOURCE: Galloway et al., 1979
Figure 78. Stratigraphic section in the South Texas uranium province

Southwest
GEOSCIENCE

Hazardous Materials Control Resources Institute (HMCRI)

Data Table

Table
Comparison of OU No. 3 Soil/Sediment Data to Regional
Background Data
RSR Corporation Superfund Site
Operable Unit No. 3

	Background Soil Concentrations (mg/kg)					Maximum - Observed OU No. 3 Concentrations (mg/kg)								
						Site 1			Site 3			Site 4		
Chemical	Range	Arithmetic Mean	Standard Deviation	Number of Samples	Arithmetic Mean + 2 Standard Deviations	Surface Soil	Sub-surface Soil	Sediment	Surface Soil	Sub-surface Soil	Sediment	Surface Soil	Sub-surface Soil	Sediment
Alummium	700 - >100,000	72,000	--	1,247	47,000	32,300	10,800	17,000	29,800	27,900	25,500	25,900	19,000	23,500
		47,000	2.48											
Arsenic	1.1 - 18	6.4	3.3	119	13	7,980	309	224	127	12.8	55.8	252	114	19.6
Barium	150 - 1,000	404	200	119	800	2,330	431	272	934	131	426	2,330	1,060	162
Berllium	N.D. - 7.0	0.62	1.06	119	2.7	4.3	0.79	2.5	1.6	1.5	2.5	2.8	1.3	2.4
Cadmium b	N.D. - 11	--	--	1,319	--	637	17.7	43.1	8.4	1.3	9.1	8.7	15.1	0.75
Chromium	3.0 - 150	40	28	119	96	204	40.5	94.1	288	85	66.6	69.1	1,420	41.7
Cobalt	N.D. - 30	4.9	4.5	119	14	86.1	21.1	12.6	19.8	32.6	64.2	264	25.7	12.6
Copper	3.0 - 30	1.5	8.0	119	31	6,610	484	219	286	37.3	213	395	2,090	71.9
Lead	N.D. - 30	1.3	8.1	119	29	105,000	6,540	3,940	71,500	320	2,100	6,390	11,500	364
Manganese b	<2.0 - 7,000	550	--	1,317	340	3,490	3,050	7,630	1,060	680	2,380	970	1,200	1,200
		330	2.77											
Mercury	<0.01 - 0.69	0.064	0.097	119	0.26	2	0.06	0.55	0.61	0.13	1.2	0.86	0.52	0.32
Nickel	N.D. - 50	12	8.8	119	30	1,180	95.1	49.4	162	12,200	62	62.6	95.8	33.2
Silver b	N.D. - 5.0	--	--	1,319	5.0	3.2	0.24	3.4	1.55	1.25	0.55	4.4	6.2	1.75
Thallium	--	--	--	--	---	4.4	1.1	7.95	0.9	2.9	1.25	2.6	5.4	2.55
Vanadium	7.0 - 200	52	37	119	130	64.7	50.2	56.3	72.8	64.7	58.8	52.1	43.7	54.3
Zinc	5.0 - 108	39	22	116	83	4,300	630	2,090	796	116	394	17,500	4,250	276

Source: Dragon. J. and Chasson Andrew, 1991. Elements in North American Soils. Hazardous Materials Control Resources Institute.

aGeometric mean

bSoil of contaminous USA, rather than Texas soils only

cMaximim value